Ultrafast relaxation dynamics in graphene

Impact of carrier-phonon and carrier-carrier scattering

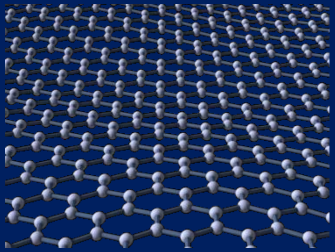

Ermin Malić, Torben Winzer, and Andreas Knorr

Technische Universität Berlin, Department for Theoretical Physics

CECAM workshop on vibrational coupling, Lausanne, November 9, 2012

Motivation

- **Density matrix formalism** offers microscopic access to **non-equilbirium dynamics** after a short-pulse excitation
- It is possible to track the way of excited carriers down to equilibrium **resolved in time, energy, and momentum**

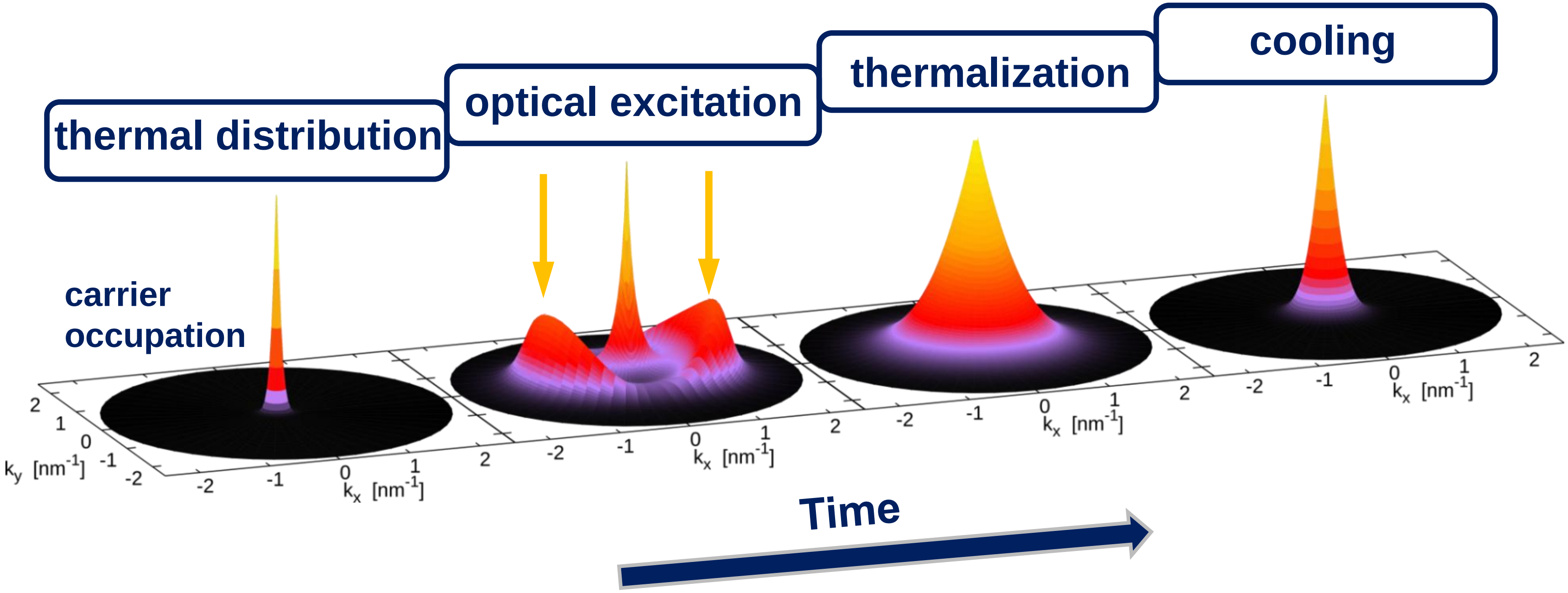

Carbon nanostructures

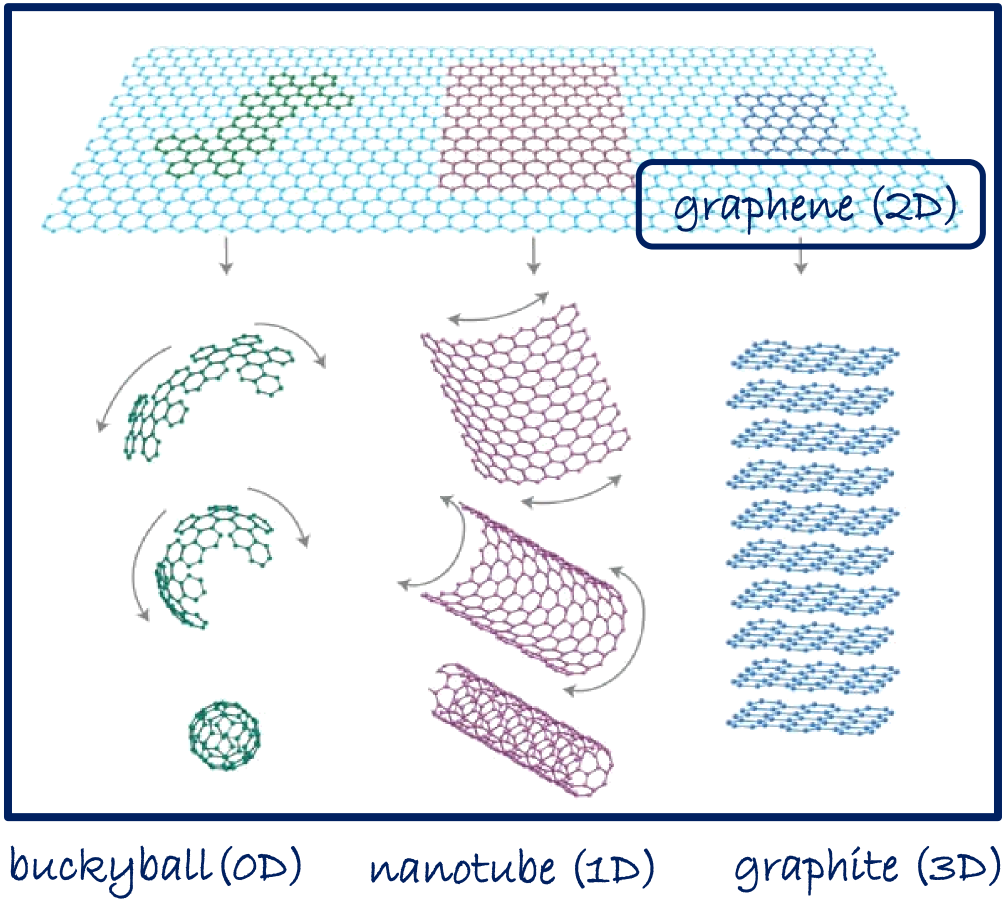

A. K. Geim and K. S. Novoselov, Nature Materials 6, 183 (2007)

Graphene

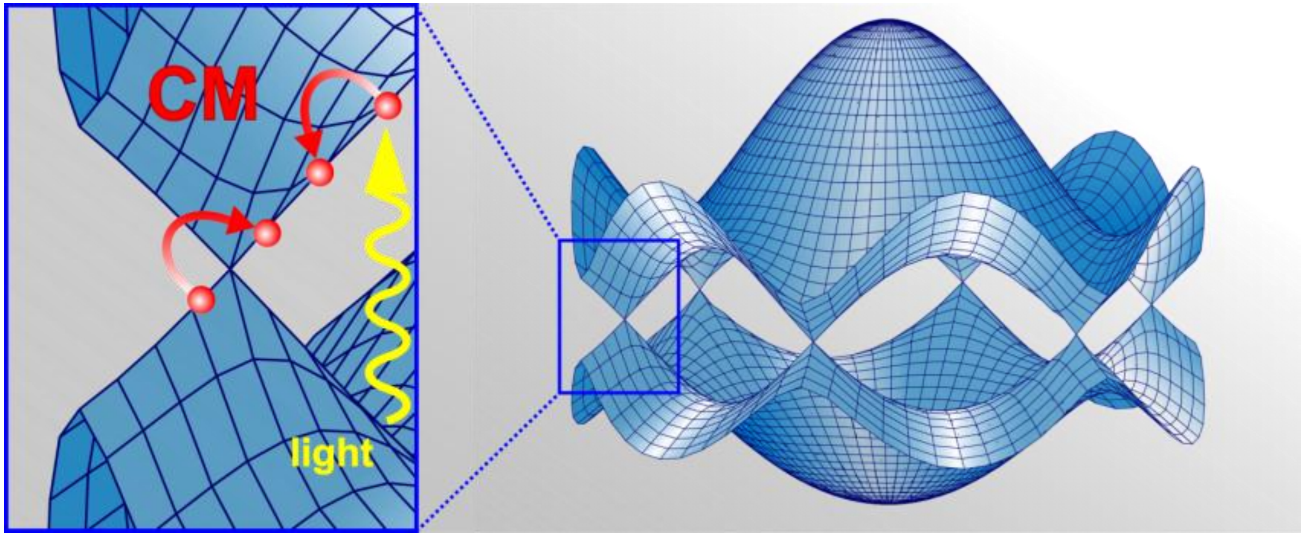

- **Graphene** is an ideal 2-dim structure to study relaxation dynamics due to its **zero-bandgap** and **linear dispersion**
- **Microscopic insights** are crucial for graphene-based **applications**

Relaxation channels

Carrier-carrier scattering

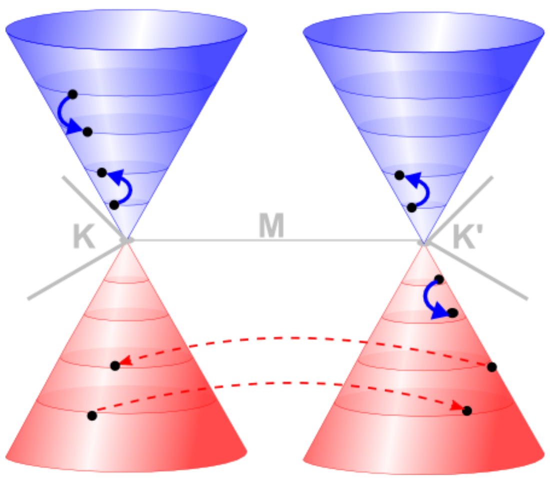

Carrier-phonon scattering

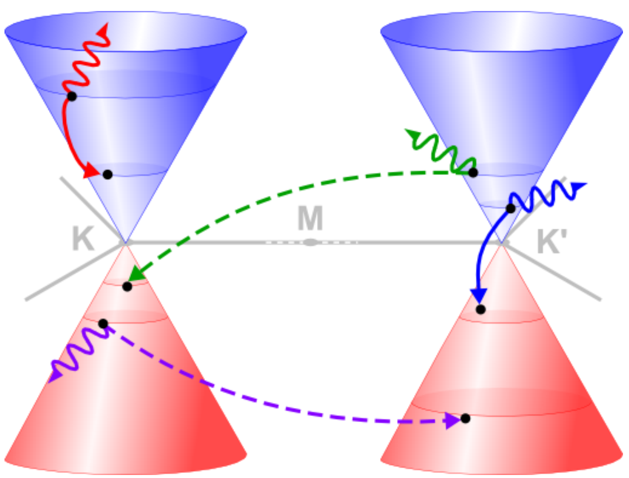

- **Intra-** and **interband scattering** channels are important
- **Auger processes** need to be taken into account
- **Intervalley scattering** via optical K phonons is efficient

Theoretical approach

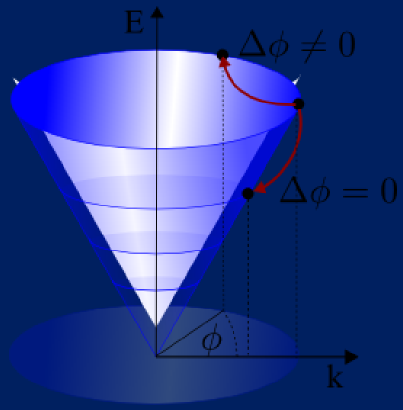

Microscopic quantities

- **Microscopic polarization** (transition probability)

  $$p_{\boldsymbol{k}}(t) = \langle a^+_{c\boldsymbol{k}} a_{v\boldsymbol{k}} \rangle$$

- **Occupation probability**

  $$\rho^\lambda_{\boldsymbol{k}}(t) = \langle a^+_{\lambda\boldsymbol{k}} a_{\lambda\boldsymbol{k}} \rangle$$

- **Phonon occupation**

  $$n^j_{\boldsymbol{q}}(t) = \langle b^+_{j\boldsymbol{q}} b_{j\boldsymbol{q}} \rangle$$

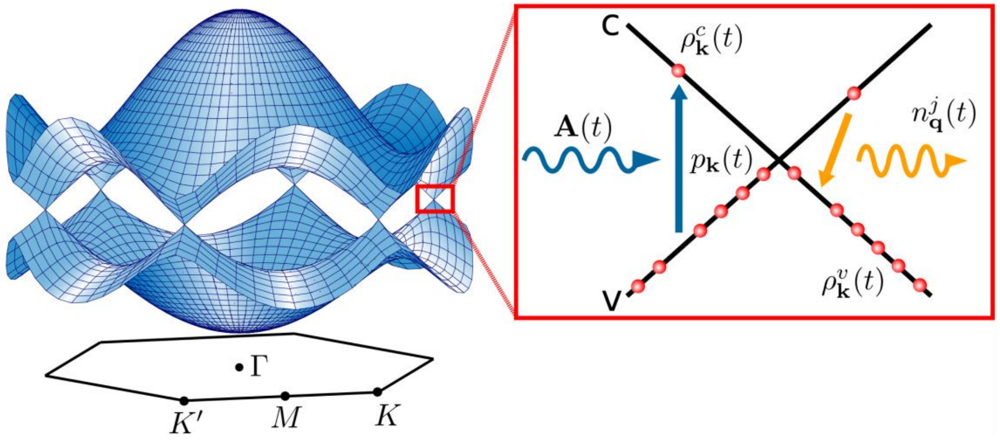

- **Second quantization** with creation and annihilation operators a^+, a and b^+, b

- Temporal evolution of quantity O(t) is determined via **Heisenberg equation** of motion

  $$i\hbar \frac{d}{dt} O(t) = [O(t), H]_-$$ ⟵ **Hamilton operator**

→ **Graphene Bloch equations** $\dot{\rho}^\lambda_{\boldsymbol{k}}, \dot{p}_{\boldsymbol{k}}, \dot{n}^j_{\boldsymbol{q}}$

Hamilton operator

$$H = H_0 + H_{c-l} + H_{c-c} + H_{c-ph}$$

free-particle **carrier-light interaction** **carrier-carrier interaction**

$$= \sum_{\boldsymbol{l}} \varepsilon_{\boldsymbol{l}} a_{\boldsymbol{l}}^{+} a_{\boldsymbol{l}} + \frac{ie_0\hbar}{m_0} \sum_{\boldsymbol{l},\boldsymbol{l'}} \boldsymbol{M}_{\boldsymbol{l},\boldsymbol{l'}} \cdot \boldsymbol{A}(t) a_{\boldsymbol{l}}^{+} a_{\boldsymbol{l'}} + \frac{1}{2} \sum_{\boldsymbol{l}_1,\boldsymbol{l}_2,\boldsymbol{l}_3,\boldsymbol{l}_4} V_{\boldsymbol{l}_3,\boldsymbol{l}_4}^{\boldsymbol{l}_1,\boldsymbol{l}_2} a_{\boldsymbol{l}_1}^{+} a_{\boldsymbol{l}_2}^{+} a_{\boldsymbol{l}_4} a_{\boldsymbol{l}_3}$$

$$+ \sum_{\boldsymbol{i}} \hbar\omega_{\boldsymbol{i}} b_{\boldsymbol{i}}^{+} b_{\boldsymbol{i}} + \sum_{\boldsymbol{l},\boldsymbol{l'}} \sum_{\boldsymbol{i}} \left(g_{\boldsymbol{l},\boldsymbol{l'}}^{\boldsymbol{i}} a_{\boldsymbol{l}}^{+} b_{\boldsymbol{i}}\, a_{\boldsymbol{l'}} + h.c. \right)$$

carrier-phonon interaction

- The required **band structure** and **matrix elements** are calculated with **tight-binding wave functions**

$$\psi_{\boldsymbol{k}}^{\lambda}(\boldsymbol{r}) = C_{\boldsymbol{k},A}^{\lambda} \Phi_{\boldsymbol{k},A}(\boldsymbol{r}) + C_{\boldsymbol{k},B}^{\lambda} \Phi_{\boldsymbol{k},B}(\boldsymbol{r})$$

$$\Phi_{\boldsymbol{k},i}(\boldsymbol{r}) = \frac{1}{\sqrt{N}} \sum_{\boldsymbol{R}_j} e^{i\boldsymbol{k}\cdot\boldsymbol{R}_j} \phi_j(\boldsymbol{r} - \boldsymbol{R}_j)$$

with **$2p_z$-orbital** functions $\phi_j(\boldsymbol{r} - \boldsymbol{R}_j)$

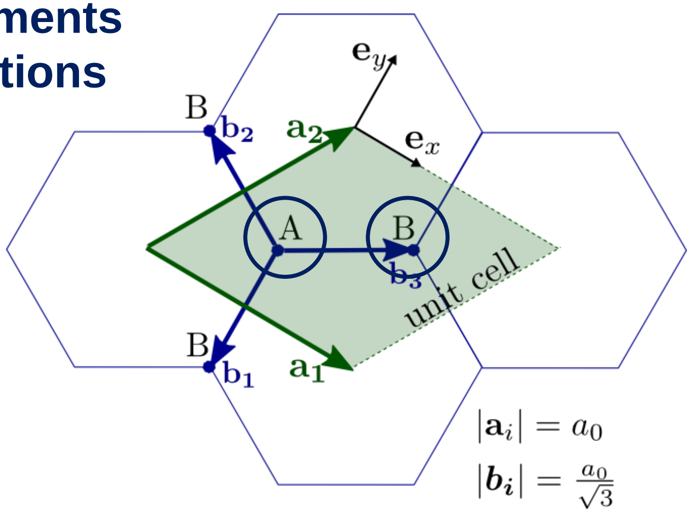

Band structure

- Solution of the **Schrödinger equation** $H\psi_{\boldsymbol{k}}^{\lambda}(\boldsymbol{r}) = \varepsilon_{\boldsymbol{k}}^{\lambda}\psi_{\boldsymbol{k}}^{\lambda}(\boldsymbol{r})$

  gives the **eigenfunction** $\psi_{\boldsymbol{k}}^{\lambda}(\boldsymbol{r})$ including the coefficients $C_{\boldsymbol{k},i}^{\lambda}$

  and the eigenvalues $\varepsilon_{\boldsymbol{k}}^{\lambda}$

- Considering contributions of **nearest-neighbor** carbon atoms yields:

$$\varepsilon_{\boldsymbol{k}}^{\lambda} =\approx \pm\hbar v_F|\boldsymbol{k}|$$

with the Fermi velocity
$v_F \approx c/300$, which can be
extracted from experiment

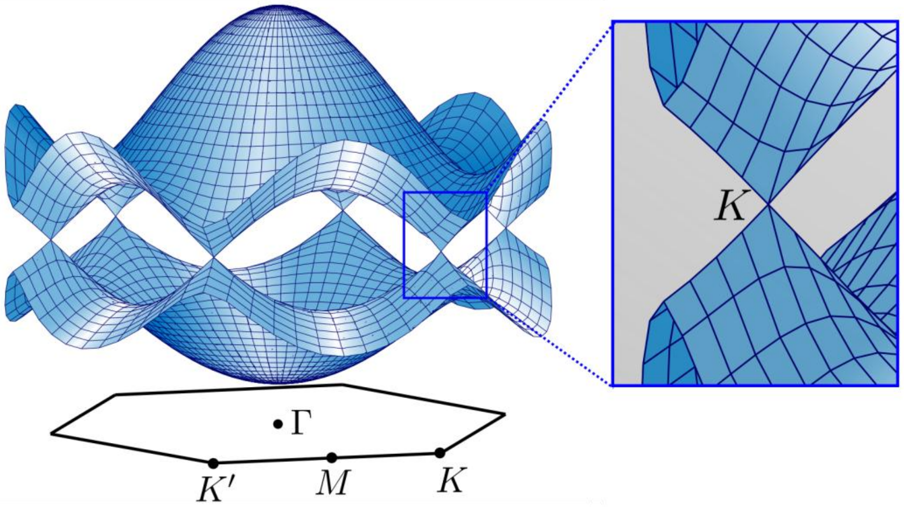

Optical matrix element

- The optical matrix element $M_{l,l'} = \langle \Psi_l(\boldsymbol{r}) \,|\, \nabla \,|\, \Psi_{l'}(\boldsymbol{r}) \rangle$ can be analytically evalutated within the **nearest-neighbor tight-binding** approximation:

$$M^{\lambda\lambda'}_{\boldsymbol{k},\boldsymbol{k'}} = \delta_{\boldsymbol{k},k'} \frac{M}{|e(\boldsymbol{k})|} \Re e \left[e^*(\boldsymbol{k}) \sum_{i=1}^{3} e^{i\boldsymbol{k}\cdot\boldsymbol{b}_i} \frac{\boldsymbol{b}_i}{|\boldsymbol{b}_i|} \right]$$

- **Carrier-light coupling** is strongly **anisotropic** around the Dirac point

- **Maximal** carrier-light interaction is found at the **M point** (saddle point)

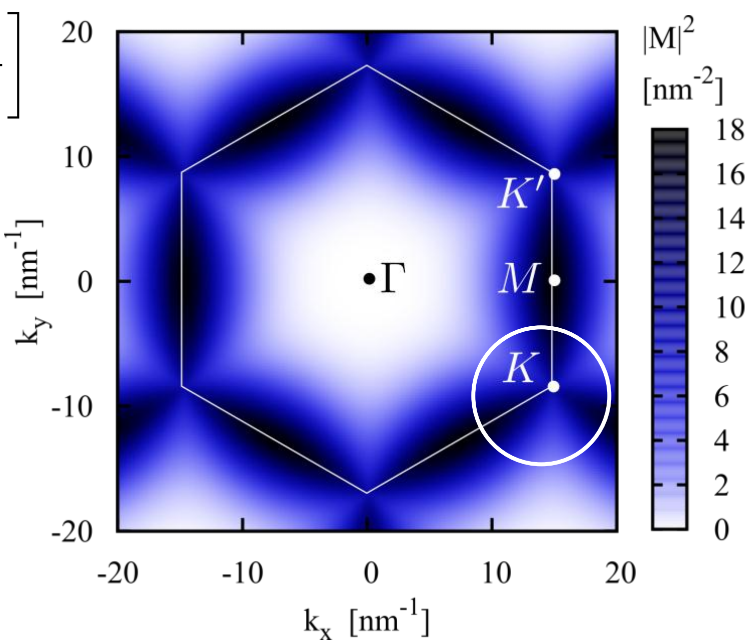

PRB 84, 205406 (2011)

Coulomb matrix element

- The Coulomb matrix element reads (with compound indices l_i=k_i, λ_i)

$$V^{\boldsymbol{l}_1,\boldsymbol{l}_2}_{\boldsymbol{l}_3,\boldsymbol{l}_4} = \int d\boldsymbol{r} \int d\boldsymbol{r}' \Psi^*_{\boldsymbol{l_1}}(\boldsymbol{r}) \Psi^*_{\boldsymbol{l_2}}(\boldsymbol{r}')\, V(\boldsymbol{r}-\boldsymbol{r}')\, \Psi_{\boldsymbol{l_4}}(\boldsymbol{r}') \Psi_{\boldsymbol{l_3}}(\boldsymbol{r})$$

- Within the **nearest-neighbor tight-binding** approximation, we obtain

$$V^{\boldsymbol{l}_1,\boldsymbol{l}_2}_{\boldsymbol{l}_3,\boldsymbol{l}_4} = \frac{e_o^2}{2\varepsilon_0 q} \left[\left(\frac{q\, a_B}{Z_{eff}} \right)^2 + 1 \right]^{-6} \alpha^{\boldsymbol{l}_1,\boldsymbol{l}_2}_{\boldsymbol{l}_3,\boldsymbol{l}_4} \boxed{\delta_{\boldsymbol{q},\boldsymbol{k}_3-\boldsymbol{k}_1} \delta_{\boldsymbol{q},\boldsymbol{k}_4-\boldsymbol{k}_2}}$$

← **momentum conservation**

with TB-coefficients $\alpha^{\boldsymbol{l}_1,\boldsymbol{l}_2}_{\boldsymbol{l}_3,\boldsymbol{l}_4} = \frac{1}{4} \left(1 + c_{\lambda_1\lambda_3} \frac{e^*(\boldsymbol{k}_1) e(\boldsymbol{k}_3)}{|e(\boldsymbol{k}_1) e(\boldsymbol{k}_3)|} \right) \left(1 + c_{\lambda_2\lambda_4} \frac{e^*(\boldsymbol{k}_2) e(\boldsymbol{k}_4)}{|e(\boldsymbol{k}_2) e(\boldsymbol{k}_4)|} \right)$

- Coulomb processes with **large momentum transfer** are **strongly suppressed** (decay scales with $\boldsymbol{1/q^{13}}$)

- Coulomb interaction $V \propto 1 \pm e^{i\Delta\phi}$ **prefers parallel intraband scattering** along the Dirac cone

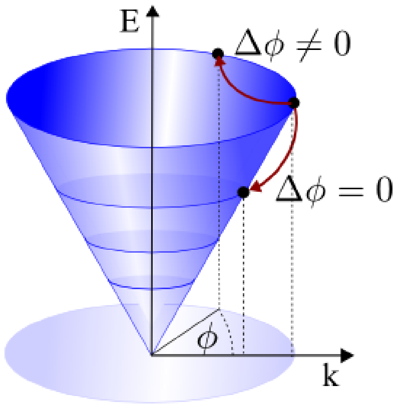

Carrier-phonon matrix element

- Focus on **strongly coupling optical phonons** (*ΓLO, ΓTO, K*)

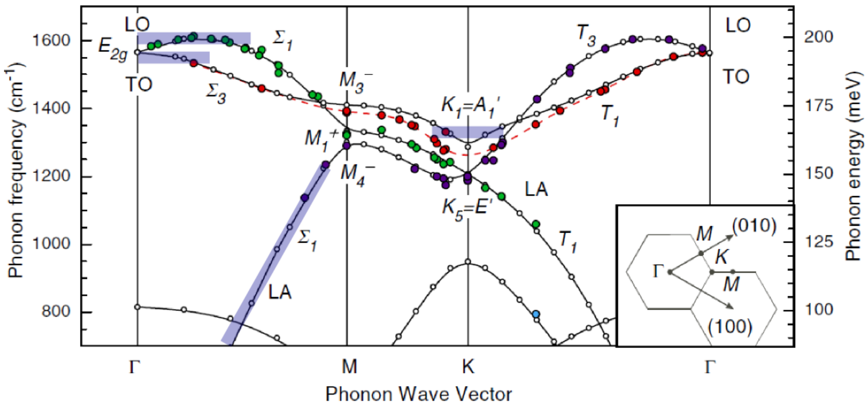

J. Maultsch et al., PRL 92, 75501 (2004)

- Carrier-phonon **matrix elements**

$$g_{\boldsymbol{q},j}^{\boldsymbol{kk}',\lambda\lambda'} = \langle \Psi_{\boldsymbol{k},\lambda}(\boldsymbol{r}) \,|\, \Delta V_{\boldsymbol{q},\gamma} \,|\, \Psi_{\boldsymbol{k}',\lambda'}(\boldsymbol{r}) \rangle$$

can be expressed as (Mauri et al.):

$$|g_{\boldsymbol{q}\Gamma j}^{\boldsymbol{kk}',\lambda\lambda'}|^2 = \frac{a_0\sqrt{3}}{2A}\tilde{g}_\Gamma^2 \left(1 + c_j^{\lambda\lambda'} cos(\phi + \phi')\right)$$

$$|g_{\boldsymbol{q}K}^{\boldsymbol{kk}',\lambda\lambda'}|^2 = \frac{a_0\sqrt{3}}{2A}\tilde{g}_K^2 \left(1 - c_K^{\lambda\lambda'} cos(\phi - \phi')\right)$$

with $\tilde{g}_\Gamma^2 = 0.0405eV^2, \tilde{g}_K^2 = 0.0994eV^2$

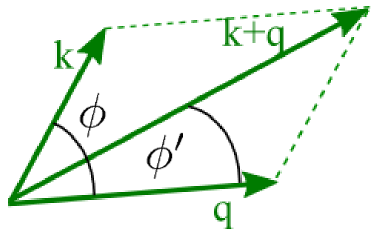

which can be extracted from experiment exploiting **Kohn anomalies**

- Phonon-induced intra- ($\lambda = \lambda$`) and interband ($\lambda \neq \lambda$`) scattering shows a distinct **angle-dependence** for different phonon modes

S. Piscanec et al., PRL 93, 185503 (2004)

Correlation expansion

- Hamilton operator H is known ⟶ derivation of **Bloch equations** $\dot{\rho}^{\lambda}_{\boldsymbol{k}}\,, \dot{p}_{\boldsymbol{k}}\,, \dot{n}^{j}_{\boldsymbol{q}}$ applying the Heisenberg equation $i\hbar\dot{\rho}^{\lambda}_{\boldsymbol{k}} = [\rho^{\lambda}_{\boldsymbol{k}}, H]_{-}$

- Many-particle interaction leads to a **hierarchy problem** (system of equations is not closed)

$$\frac{d}{dt}\langle a_1^{+} a_2 \rangle \;\propto\; \langle a_A^{+} a_B^{+} a_C a_D \rangle$$

$$\frac{d}{dt}\langle a_A^{+} a_B^{+} a_C a_D \rangle \;\propto\; \langle a_1^{+} a_2^{+} a_3^{+} a_4\, a_5\, a_6 \rangle \quad \ldots$$

- Solution by applying the **correlation expansion** and systematic truncation

Example: **Hartree-Fock** factorization (single-particle quantities only)

$$\langle a_A^{+} a_B^{+} a_C a_D \rangle = \langle a_A^{+} a_D \rangle \langle a_B^{+} a_C \rangle - \langle a_A^{+} a_C \rangle \langle a_B^{+} a_D \rangle + \langle a_A^{+} a_B^{+} a_C a_D \rangle^{c}$$

⟶ **closed system of equations** (already sufficient for description of **excitons**)

Markov approximation

- For description of **scattering processes**, dynamics of two-particle quantities is necessary $\sigma_{ABCD} = \langle a_A^+ a_B^+ a_C a_D \rangle$ (**second-order Born**)

$$\frac{d}{dt}\sigma_{ABCD}(t) = \frac{i}{\hbar}\Delta\varepsilon\,\sigma_{ABCD}(t) + \frac{i}{\hbar}Q(t) - \gamma\,\sigma_{ABCD}(t)$$

with the scattering term *Q(t)* including only single-particle quantities

- Für 2-dim systems, such as graphene with $A = (k_x, k_y, \lambda)$, the evaluation of equations is a **numerical challenge** (memory, CPU time)

- **Markov approximation** neglects quantum-kinetic memory effects:

$$\sigma_{ABCD}(t) = \frac{i}{\hbar}\int_0^\infty e^{\left(\frac{i}{\hbar}\Delta\varepsilon+\gamma\right)s}\,Q(t-s)\,ds \quad \approx \quad -i\pi\,Q(t)\,\delta(\Delta\varepsilon) \qquad (\gamma \to 0)$$

→ **closed system of equations**

Graphene Bloch equations

- Dynamics of **carriers**, **phonons,** and microscopic **polarization** within **second order Born-Markov** approximation

$$\dot{\rho}^{\lambda}_{\mathbf{k}}(t) = 2\mathrm{Im}\left(\Omega^{*}_{\mathrm{k}}(\mathrm{t})\mathrm{p}_{\mathrm{k}}(\mathrm{t})\right) + \Gamma^{in}_{\boldsymbol{k},\lambda}(t)\left(1-\rho^{\lambda}_{\boldsymbol{k}}(t)\right) - \Gamma^{out}_{\boldsymbol{k},\lambda}(t)\rho^{\lambda}_{\boldsymbol{k}}(t)$$

$$\dot{p}_{\mathbf{k}}(t) = -i\omega_{\boldsymbol{k}}p_{\boldsymbol{k}}(t) - i\Omega_{\boldsymbol{k}}(t)\left(\rho^{c}_{\boldsymbol{k}}(t)-\rho^{v}_{\boldsymbol{k}}(t)\right) - \gamma_{2,\boldsymbol{k}}(t)\,p_{\boldsymbol{k}}(t) + \tilde{\gamma}_{2,\boldsymbol{k}'}(t)$$

$$\dot{n}^{j}_{\mathbf{q}}(t) = \Gamma^{out}_{j,\mathbf{q}}(t)\left(n^{j}_{\mathbf{q}}(t)+1\right) - \Gamma^{in}_{j,\mathbf{q}}(t)n^{j}_{\mathbf{q}}(t) - \gamma_j(n^{j}_{\boldsymbol{q}}(t)-n_0)$$

$$H = H_0 + H_{c-l} + H_{c-c} + H_{c-ph}$$

- **Carrier-light** coupling describes the generation of **optically excited non-equilibrium** carrier distribution

Nano Lett. 10, 489 (2010) ; PRB 84, 205406 (2011)

Graphene Bloch equations

- Dynamics of **carriers**, **phonons,** and microscopic **polarization** within **second order Born-Markov** approximation:

$$\dot{\rho}^{\lambda}_{\mathbf{k}}(t) = 2\mathrm{Im}\left(\Omega^{*}_{\mathrm{k}}(\mathrm{t})\mathrm{p}_{\mathrm{k}}(\mathrm{t})\right) + \Gamma^{in}_{\boldsymbol{k},\lambda}(t)\left(1-\rho^{\lambda}_{\boldsymbol{k}}(t)\right) - \Gamma^{out}_{\boldsymbol{k},\lambda}(t)\rho^{\lambda}_{\boldsymbol{k}}(t)$$

$$\dot{p}_{\mathbf{k}}(t) = -i\omega_{\boldsymbol{k}}p_{\boldsymbol{k}}(t) - i\Omega_{\boldsymbol{k}}(t)\left(\rho^{c}_{\boldsymbol{k}}(t)-\rho^{v}_{\boldsymbol{k}}(t)\right) - \gamma_{2,\boldsymbol{k}}(t)\,p_{\boldsymbol{k}}(t) + \tilde{\gamma}_{2,\boldsymbol{k}'}(t)$$

$$\dot{n}^{j}_{\mathbf{q}}(t) = \Gamma^{out}_{j,\mathbf{q}}(t)\left(n^{j}_{\mathbf{q}}(t)+1\right) - \Gamma^{in}_{j,\mathbf{q}}(t)n^{j}_{\mathbf{q}}(t) - \gamma_{j}(n^{j}_{\boldsymbol{q}}(t)-n_{0})$$

- **Time-, momentum-,** and **angle-resolved** Coulomb and phonon scattering rates $\Gamma^{in}_{\boldsymbol{k},\lambda} = \Gamma^{in,cc}_{\boldsymbol{k},\lambda} + \Gamma^{in,cp}_{\boldsymbol{k},\lambda}$

$$\Gamma^{in,cc}_{\boldsymbol{k},\lambda} = \frac{2\pi}{\hbar}\sum_{\boldsymbol{l_1},\boldsymbol{l_2},\boldsymbol{l_3}} W^{\boldsymbol{k}\lambda\,\boldsymbol{l_1}\,*}_{\boldsymbol{l_2}\,\boldsymbol{l_3}}\left(2W^{\boldsymbol{k}\lambda\,\boldsymbol{l_1}\,*}_{\boldsymbol{l_2}\,\boldsymbol{l_3}} - W^{\boldsymbol{k}\lambda\,\boldsymbol{l_1}\,*}_{\boldsymbol{l_3}\,\boldsymbol{l_2}}\right)\rho_{\boldsymbol{l_2}}\rho_{\boldsymbol{l_3}}(1-\rho_{\boldsymbol{l_1}})\delta(\varepsilon_{\boldsymbol{k}\lambda}+\varepsilon_{\boldsymbol{l_1}}-\varepsilon_{\boldsymbol{l_2}}-\varepsilon_{\boldsymbol{l_3}})$$

screened Coulomb matrix elements ↗ **Pauli blocking** ↗

Nano Lett. 10, 489 (2010) ; PRB 84, 205406 (2011)

Graphene Bloch equations

- Dynamics of **carriers**, **phonons,** and microscopic **polarization** within **second order Born-Markov** approximation:

$$\dot{\rho}^{\lambda}_{\mathbf{k}}(t) = 2\mathrm{Im}\left(\Omega^{*}_{\mathrm{k}}(\mathrm{t})\mathrm{p}_{\mathrm{k}}(\mathrm{t})\right) + \Gamma^{in}_{\boldsymbol{k},\lambda}(t)\left(1-\rho^{\lambda}_{\boldsymbol{k}}(t)\right) - \Gamma^{out}_{\boldsymbol{k},\lambda}(t)\rho^{\lambda}_{\boldsymbol{k}}(t)$$

$$\dot{p}_{\mathbf{k}}(t) = -i\omega_{\boldsymbol{k}}p_{\boldsymbol{k}}(t) - i\Omega_{\boldsymbol{k}}(t)\left(\rho^{c}_{\boldsymbol{k}}(t)-\rho^{v}_{\boldsymbol{k}}(t)\right) - \gamma_{2,\boldsymbol{k}}(t)\,p_{\boldsymbol{k}}(t) + \tilde{\gamma}_{2,\boldsymbol{k}'}(t)$$

$$\dot{n}^{j}_{\mathbf{q}}(t) = \Gamma^{out}_{j,\mathbf{q}}(t)\left(n^{j}_{\mathbf{q}}(t)+1\right) - \Gamma^{in}_{j,\mathbf{q}}(t)n^{j}_{\mathbf{q}}(t) - \gamma_{j}(n^{j}_{\boldsymbol{q}}(t)-n_{0})$$

- **Time-, momentum-,** and **angle-resolved** Coulomb and phonon scattering rates $\Gamma^{in}_{\boldsymbol{k},\lambda} = \Gamma^{in,cc}_{\boldsymbol{k},\lambda} + \Gamma^{in,cp}_{\boldsymbol{k},\lambda}$

$$\Gamma^{in,cp}_{\boldsymbol{k},\lambda} = \sum_{\boldsymbol{q},j,\lambda'} |g^{\boldsymbol{k}\boldsymbol{k}',\lambda\lambda'}_{\boldsymbol{q},j}|^{2} f^{\lambda'}_{\boldsymbol{k}+\boldsymbol{q}}\Big((n^{j}_{\boldsymbol{q}}+1)\delta(\varepsilon_{\boldsymbol{k}+\boldsymbol{q},\lambda'}-\varepsilon_{\boldsymbol{k},\lambda}-\hbar\omega_{\boldsymbol{q},j}) + n^{j}_{\boldsymbol{q}}\delta(\varepsilon_{\boldsymbol{k}+\boldsymbol{q},\lambda'}-\varepsilon_{\boldsymbol{k},\lambda}+\hbar\omega_{\boldsymbol{q},j})\Big)$$

phonon emission **phonon absorption**

Nano Lett. 10, 489 (2010) ; PRB 84, 205406 (2011)

Graphene Bloch equations

- Dynamics of **carriers**, **phonons,** and microscopic **polarization** within **second order Born-Markov** approximation:

$$\dot{\rho}^{\lambda}_{\mathbf{k}}(t) = 2\mathrm{Im}\left(\Omega^*_{\mathrm{k}}(\mathrm{t})\mathrm{p}_{\mathrm{k}}(\mathrm{t})\right) + \Gamma^{in}_{\boldsymbol{k},\lambda}(t)\left(1-\rho^{\lambda}_{\boldsymbol{k}}(t)\right) - \Gamma^{out}_{\boldsymbol{k},\lambda}(t)\rho^{\lambda}_{\boldsymbol{k}}(t)$$

$$\dot{p}_{\mathbf{k}}(t) = -i\omega_{\boldsymbol{k}}p_{\boldsymbol{k}}(t) - i\Omega_{\boldsymbol{k}}(t)\left(\rho^{c}_{\boldsymbol{k}}(t)-\rho^{v}_{\boldsymbol{k}}(t)\right) - \gamma_{2,\boldsymbol{k}}(t)\,p_{\boldsymbol{k}}(t) + \tilde{\gamma}_{2,\boldsymbol{k}'}(t)$$

$$\dot{n}^{j}_{\mathbf{q}}(t) = \Gamma^{out}_{j,\mathbf{q}}(t)\left(n^{j}_{\mathbf{q}}(t)+1\right) - \Gamma^{in}_{j,\mathbf{q}}(t)n^{j}_{\mathbf{q}}(t) - \gamma_j\left(n^{j}_{\boldsymbol{q}}(t)-n_0\right)$$

- **Time-, momentum-,** and **angle-resolved** Coulomb and phonon scattering rates $\Gamma^{in}_{\boldsymbol{k},\lambda} = \Gamma^{in,cc}_{\boldsymbol{k},\lambda} + \Gamma^{in,cp}_{\boldsymbol{k},\lambda}$

- **Diagonal** and **off-diagonal dephasing** of the microscopic polarization

$$\gamma_{2,\boldsymbol{k}}(t) = \frac{1}{2}\sum_{\lambda}\left(\Gamma^{in}_{\boldsymbol{k},\lambda}(t)+\Gamma^{out}_{\boldsymbol{k},\lambda}(t)\right),\ \tilde{\gamma}_{2,\boldsymbol{k}}(t) = \sum_{\boldsymbol{k}'}\left(T^{a}_{\boldsymbol{k}\boldsymbol{k}'}(t)p_{\boldsymbol{k}'}(t) + T^{b}_{\boldsymbol{k}\boldsymbol{k}'}(t)p^{*}_{\boldsymbol{k}'}(t)\right)$$

Nano Lett. 10, 489 (2010) ; PRB 84, 205406 (2011)

Outline

- Anisotropy, thermalization, and cooling
- Auger-induced carrier multiplication
- Transient optical gain

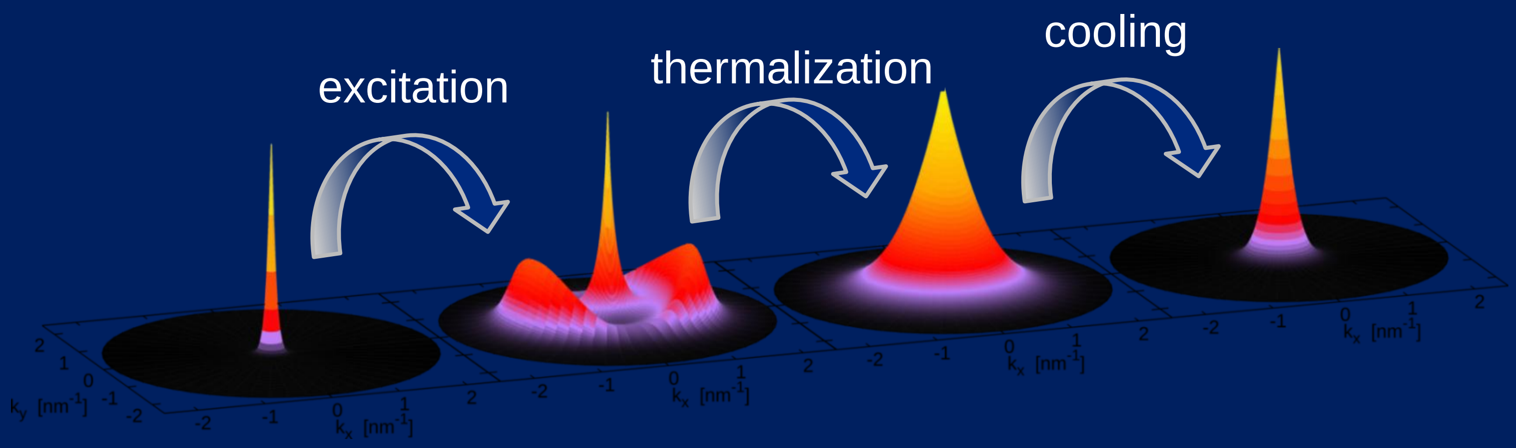

Generation of a non-equilibrium

- **Optical excitation** according to a recent **experiment** (T. Elsaesser, MBI Berlin):
  - pulse width **10 fs**
  - excitation energy **1.5 eV**
  - pump fluence **1 μJcm^{-2}**
  - **linear** polarization (x-axis)

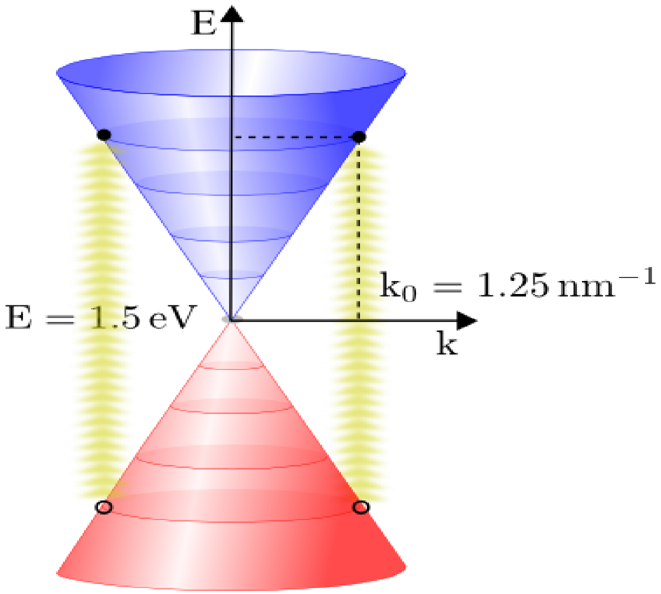

Generation of a non-equilibrium

- **Optical excitation** according to a recent **experiment** (T. Elsaesser, MBI Berlin):
  - pulse width **10 fs**
  - excitation energy **1.5 eV**
  - pump fluence **1 μJcm^{-2}**
  - **linear** polarization (x-axis)

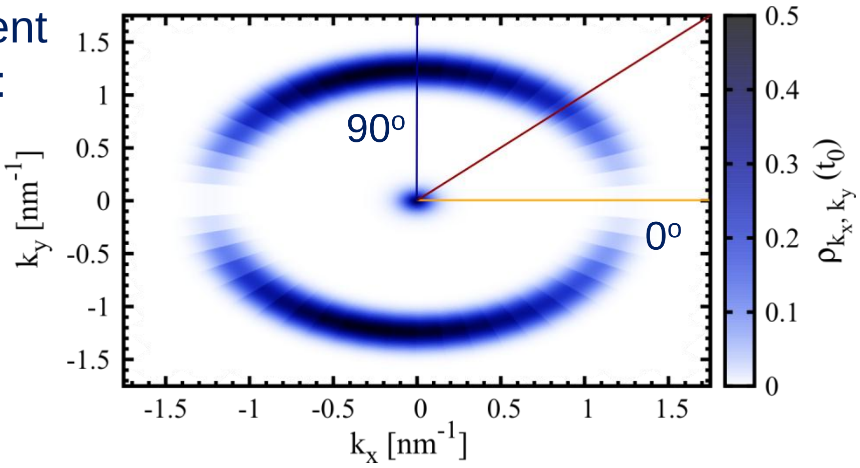

- Generation of an **anisotropic non-equilibrium** carrier distribution
- **Maximal occupation** perpendicular to polarization of excitation pulse (**90º**)
- Origin lies in the **anisotropy** of the **carrier-light coupling** element

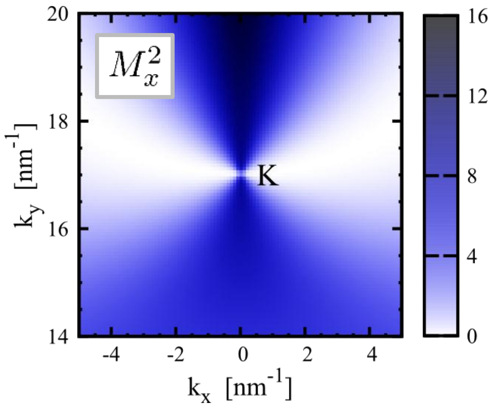

PRB 84, 205406 (2011)

Anisotropic non-equilibrium

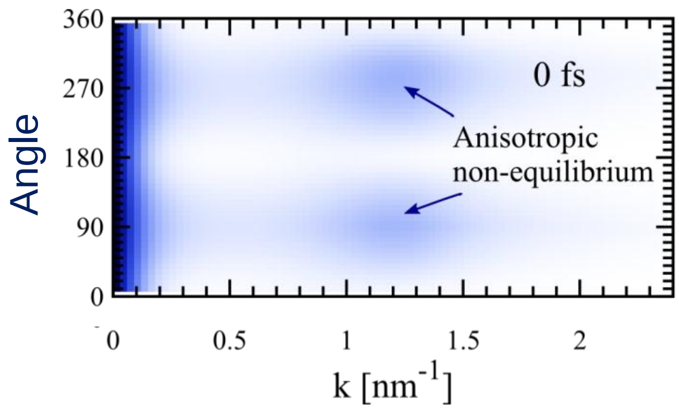

- Generation of an **anisotropic non-equilibrium** carrier distribution

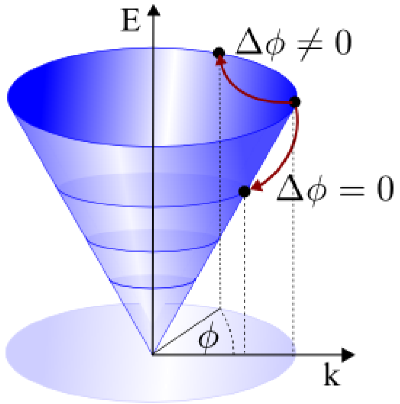

Orientational relaxation

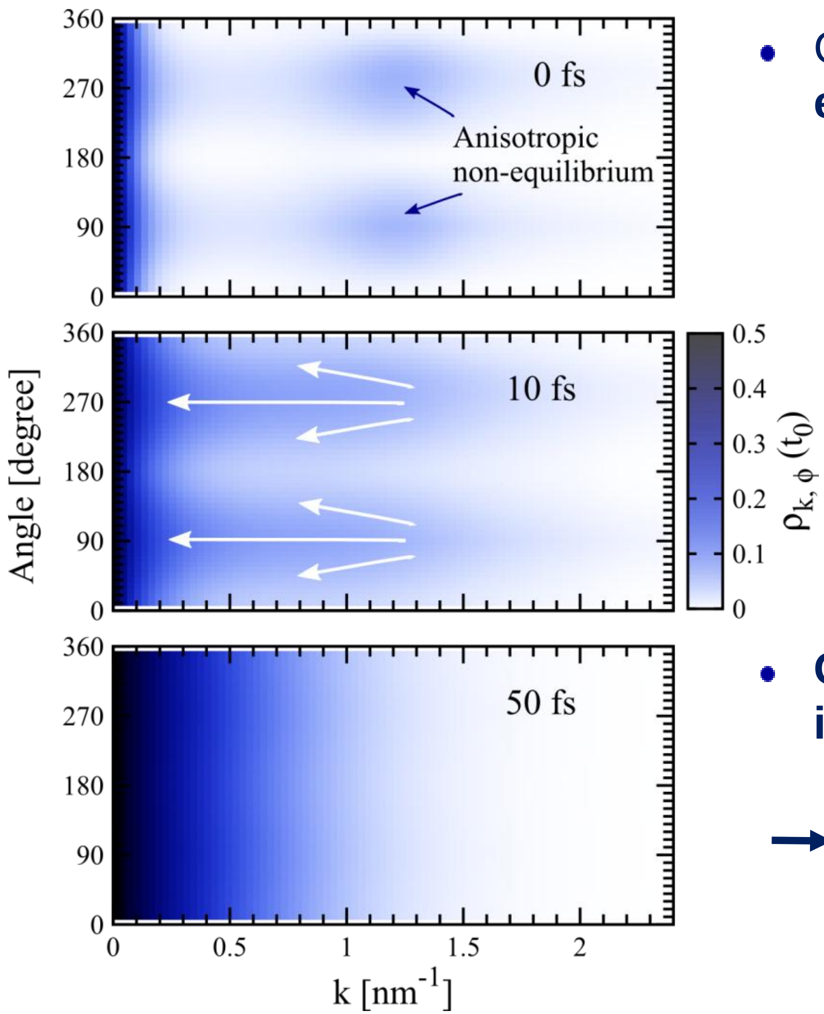

- Generation of an **anisotropic non-equilibrium** carrier distribution

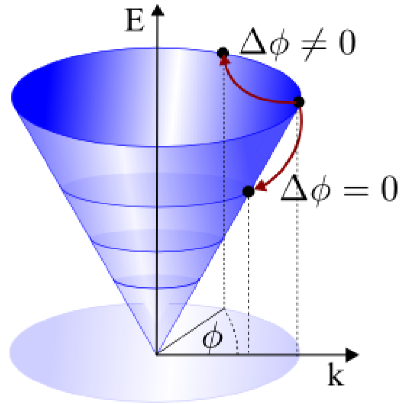

- **Orientational relaxation** accounts for **isotropy** already after **50 fs**

→ Good **agreement** with recent **experiments** (H. Kurz, RWTH Aachen
A. Hartschuh, LMU München)

APL , in print (2012)

Carrier-carrier vs. carrier-phonon

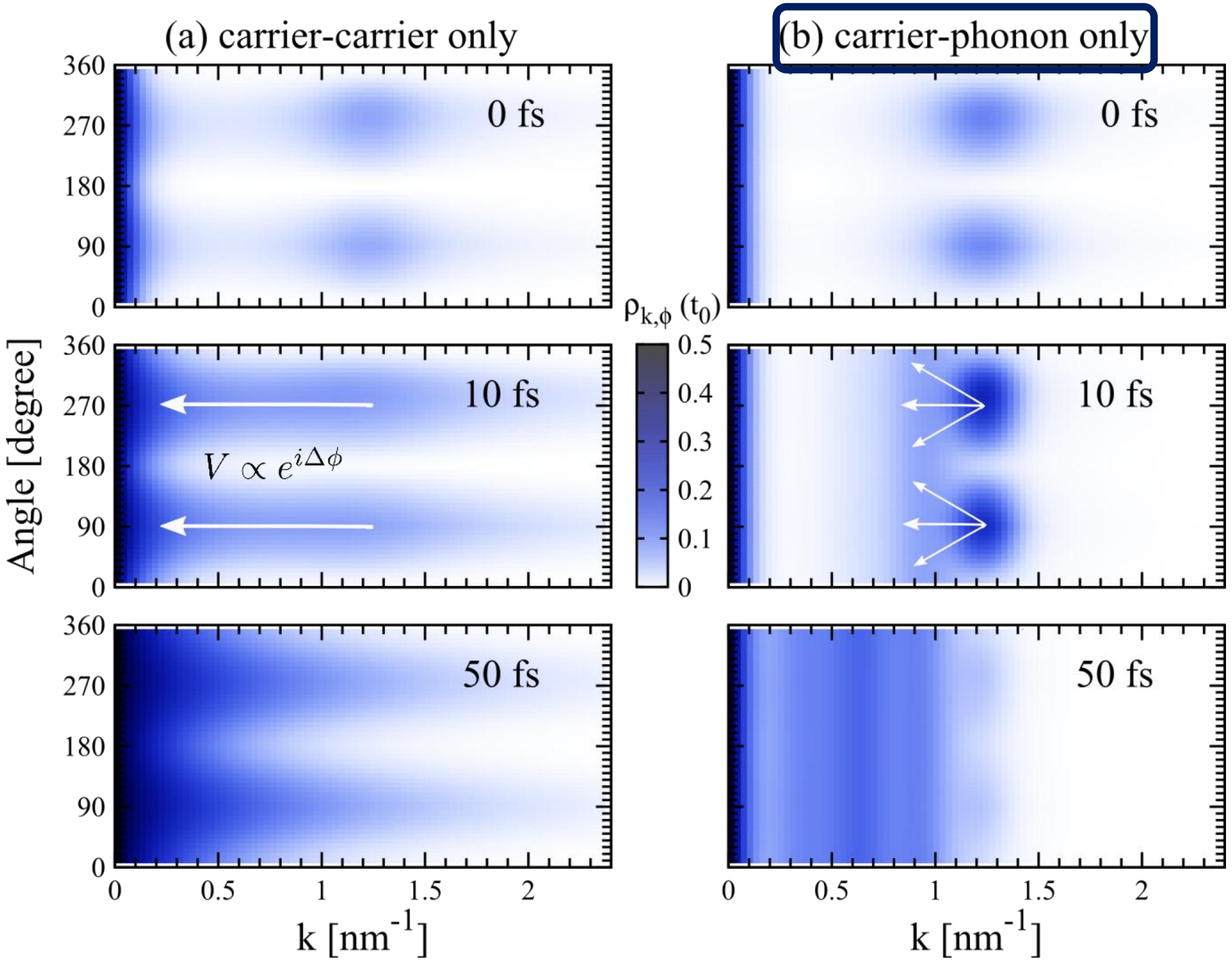

Different phonon modes

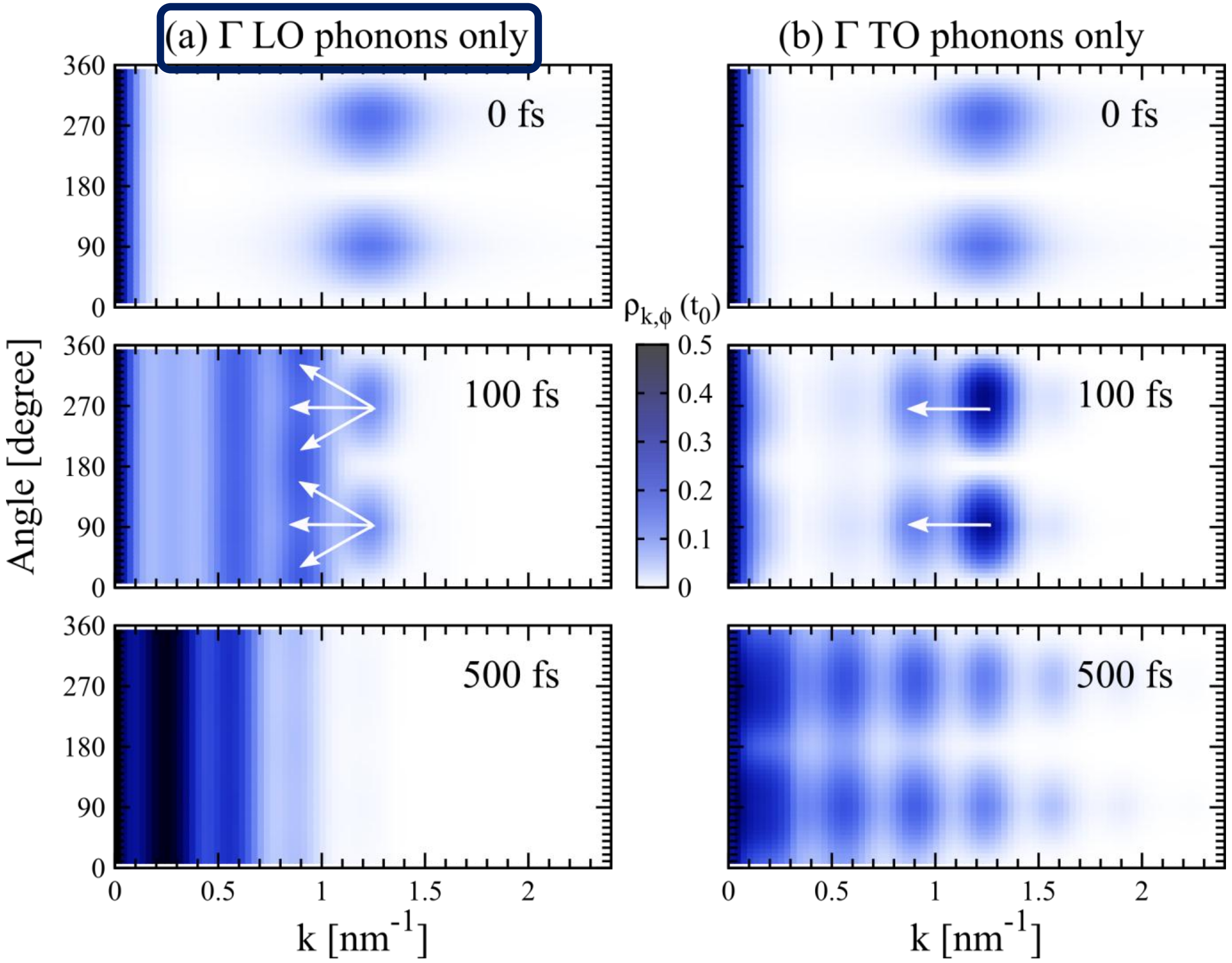

Phonon dynamics

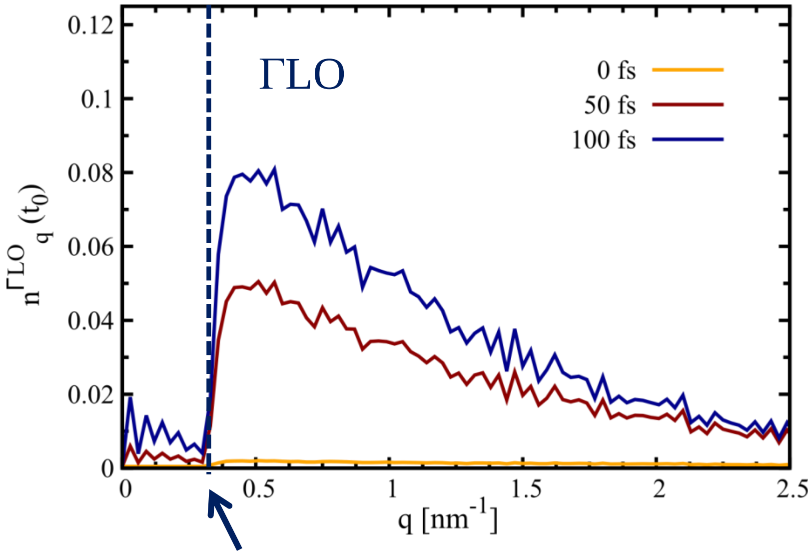

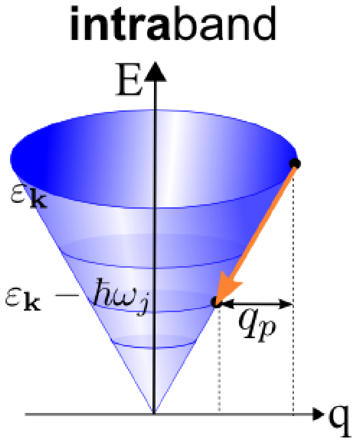

q_p || k: parallel scattering with $q_p = \frac{\omega_{\Gamma LO}}{\nu_F}$
(conserves anisotrop)

Phonon dynamics

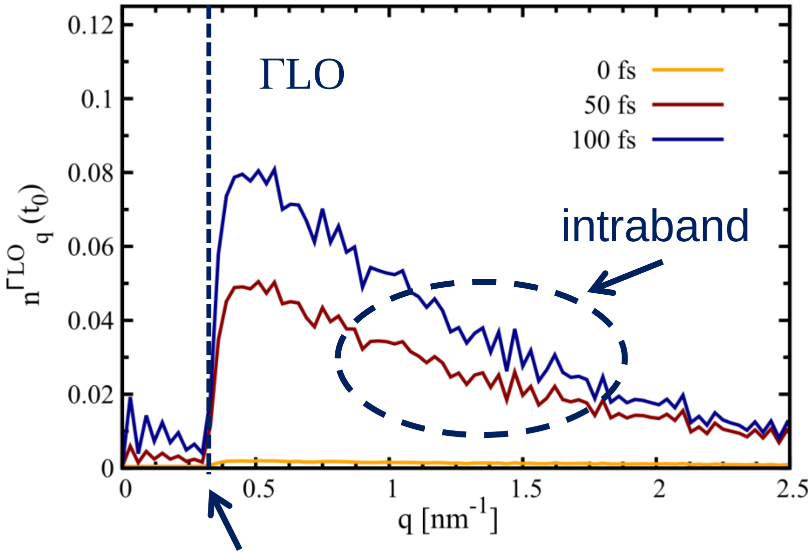

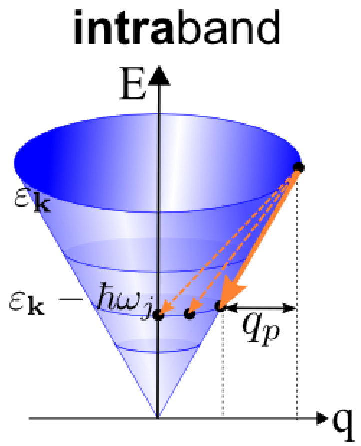

$$|g^{\boldsymbol{kk'},\lambda\lambda}_{\boldsymbol{q}\Gamma LO}|^2 = \frac{a_0\sqrt{3}}{2A}\tilde{g}^2_\Gamma\,(1 - cos(\phi + \phi'))$$

q_p || k: parallel scattering with $q_p = \frac{\omega_{\Gamma LO}}{\nu_F}$
(conserves anisotrop)

- **ΓLO phonons** prefer **intraband** scattering across the Dirac cone with $q > q_p$

→ **isotropic** carrier distribution

PRB 84, 205406 (2011)

Phonon dynamics

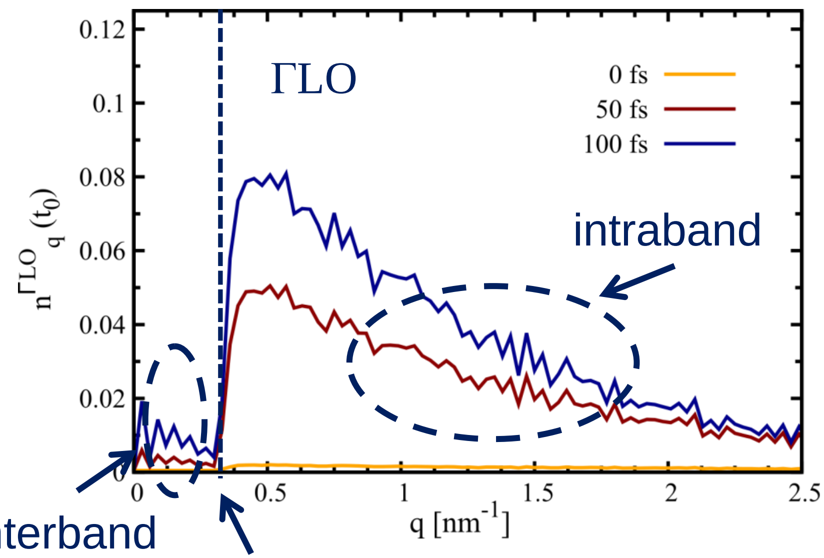

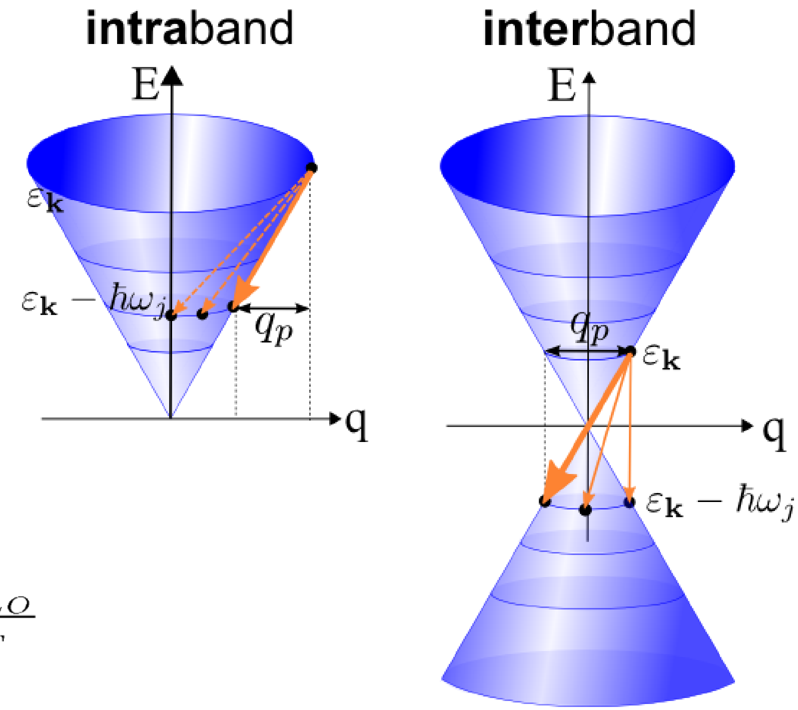

q_p || k: parallel scattering with $q_p = \frac{\omega_{\Gamma LO}}{\nu_F}$
(conserves anisotrop)

- **ΓLO phonons** prefer **intraband** scattering across the Dirac cone with $q > q_p$

→ **isotropic** carrier distribution

PRB 84, 205406 (2011)

Phonon dynamics

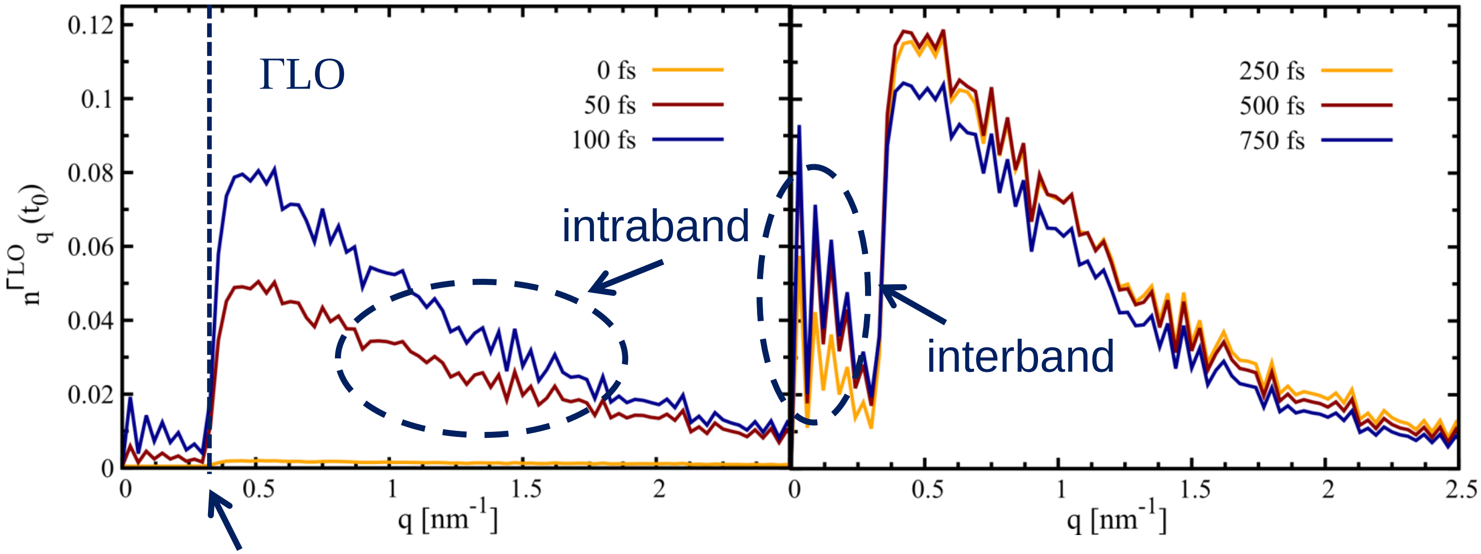

q_p || k: parallel scattering with $q_p = \frac{\omega_{\Gamma LO}}{\nu_F}$
(conserves anisotrop)

- **ΓLO phonons** prefer **intraband** scattering across the Dirac cone with $q > q_p$
  → **isotropic** carrier distribution
- **Interband** processes with $q < q_p$ important **at later times** (carrier recombination)

PRB 84, 205406 (2011)

Phonon dynamics

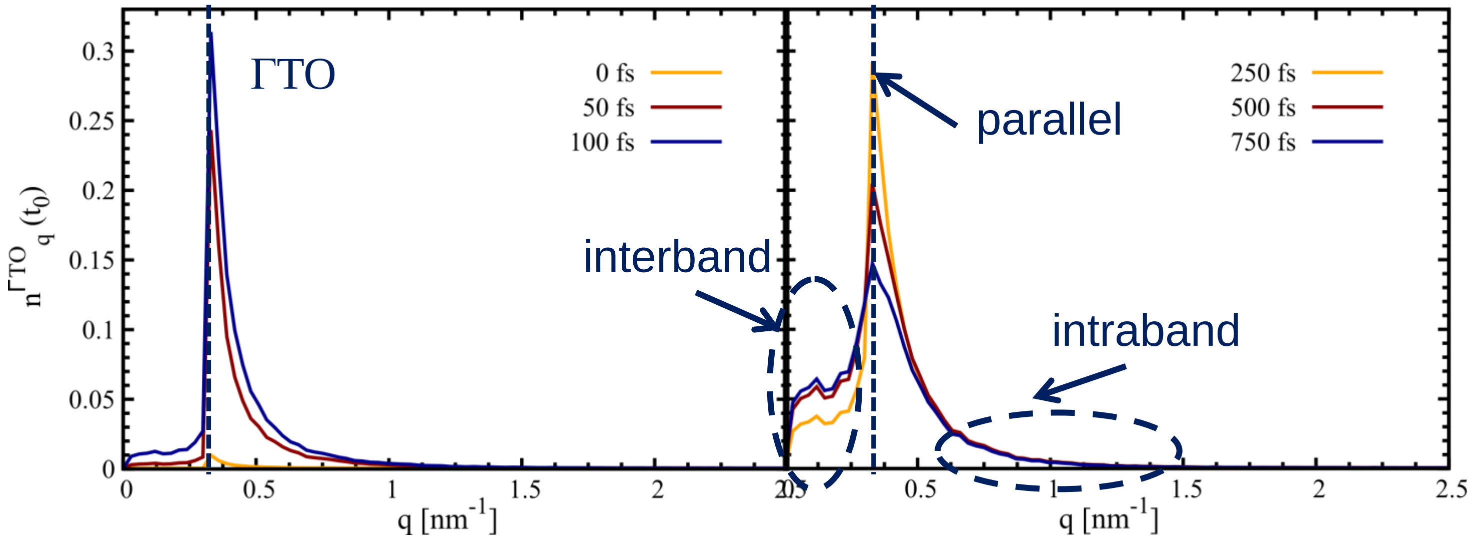

$$|g_{\boldsymbol{q}\Gamma TO}^{\boldsymbol{kk}',\lambda\lambda}|^2 = \frac{a_0\sqrt{3}}{2A}\tilde{g}_\Gamma^2\,(1 + cos(\phi + \phi'))$$

- **ΓTO phonons** strongly prefer **parallel scattering** along the Dirac cone conserving the initial **anisotropy**
- They contribute to an ultrafast **carrier thermalization** and **cooling**

Phonons account for isotropy

- **Carrier-phonon** coupling is **efficient** for scattering **across** the Dirac cone $\Delta\phi \neq 0$

  → **isotropic** distribution

- Carrier-carrier and carrier-phonon **channels in competition** for scattering **along** the Dirac cone $\Delta\phi = 0$

  → **thermalization**

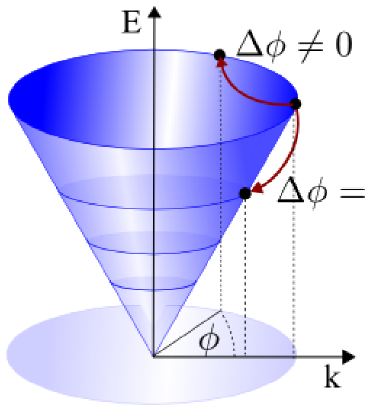

→ **Challenge**:

Impact of **Non-Markov** scattering processes

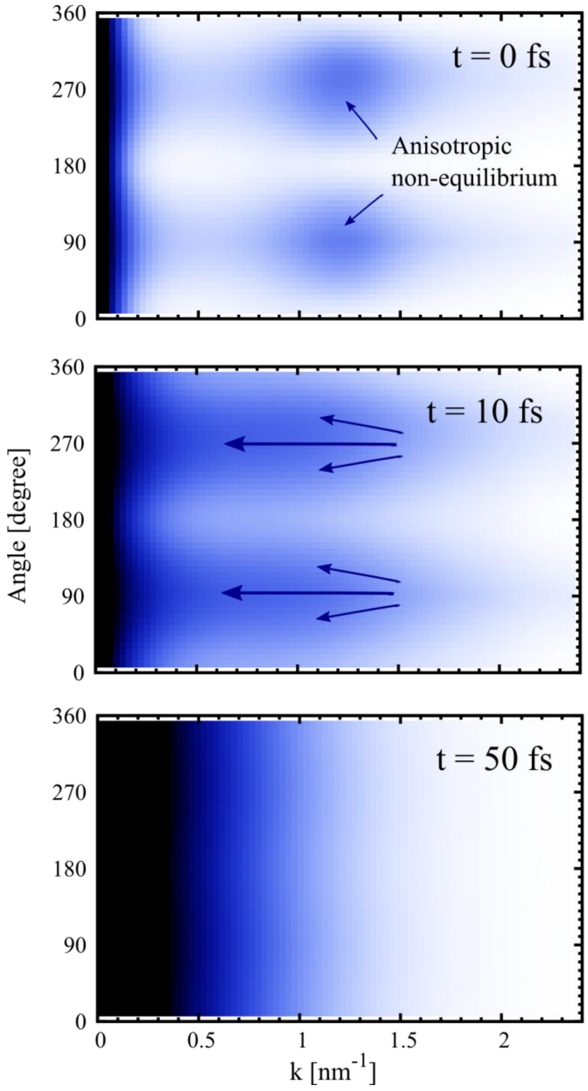

APL, in press (2012), PRB 84, 205406 (2011)

Thermalization

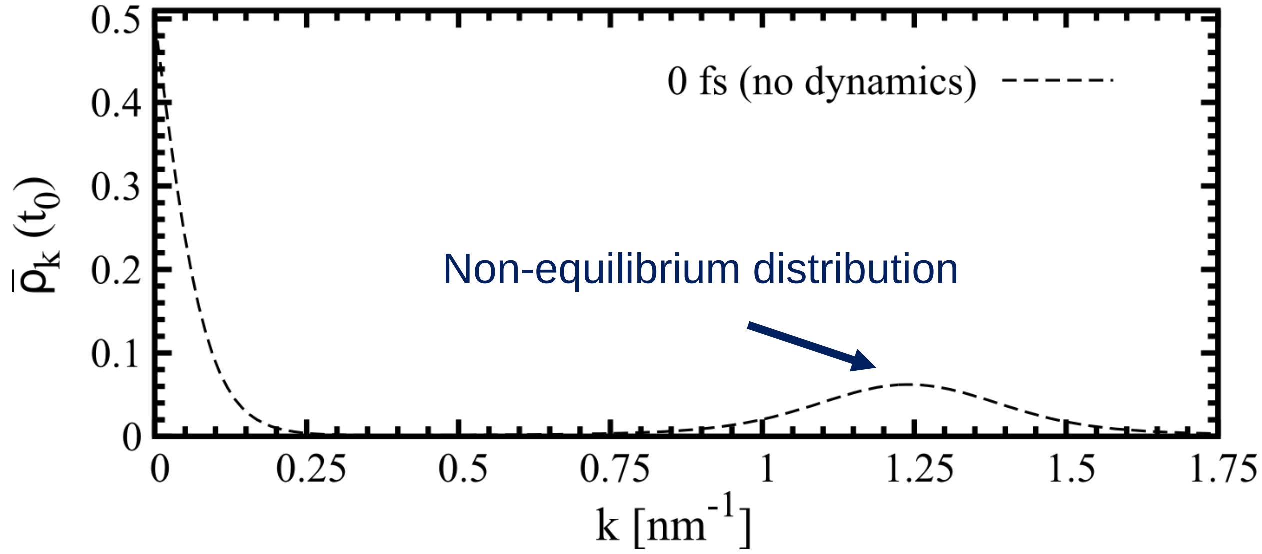

Thermalization

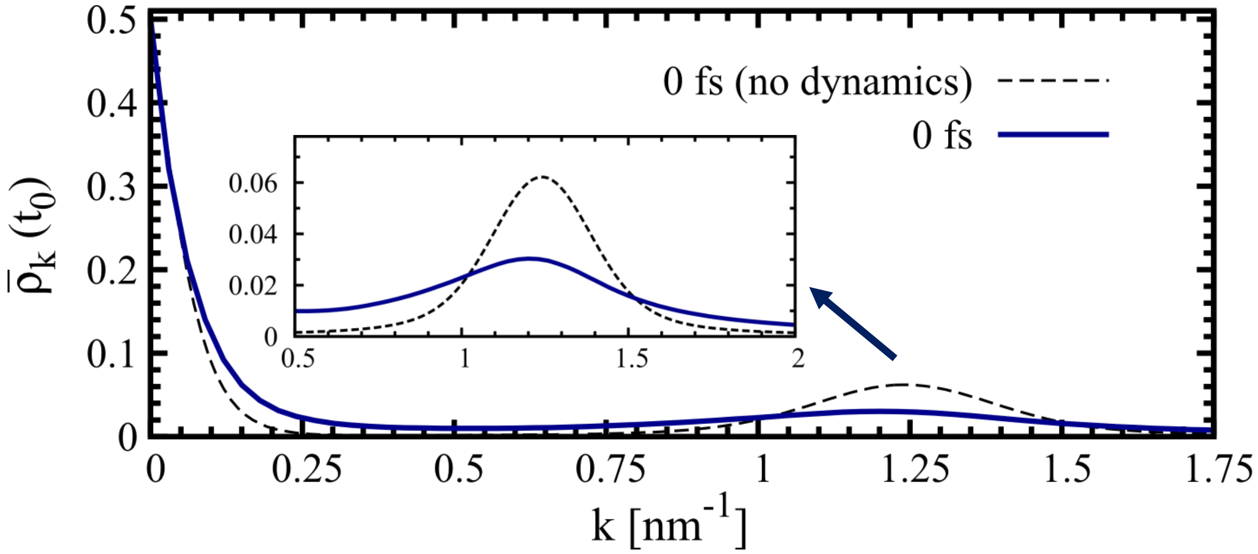

- Significant **relaxation** takes place already **during** the excitation **pulse**

Thermalization

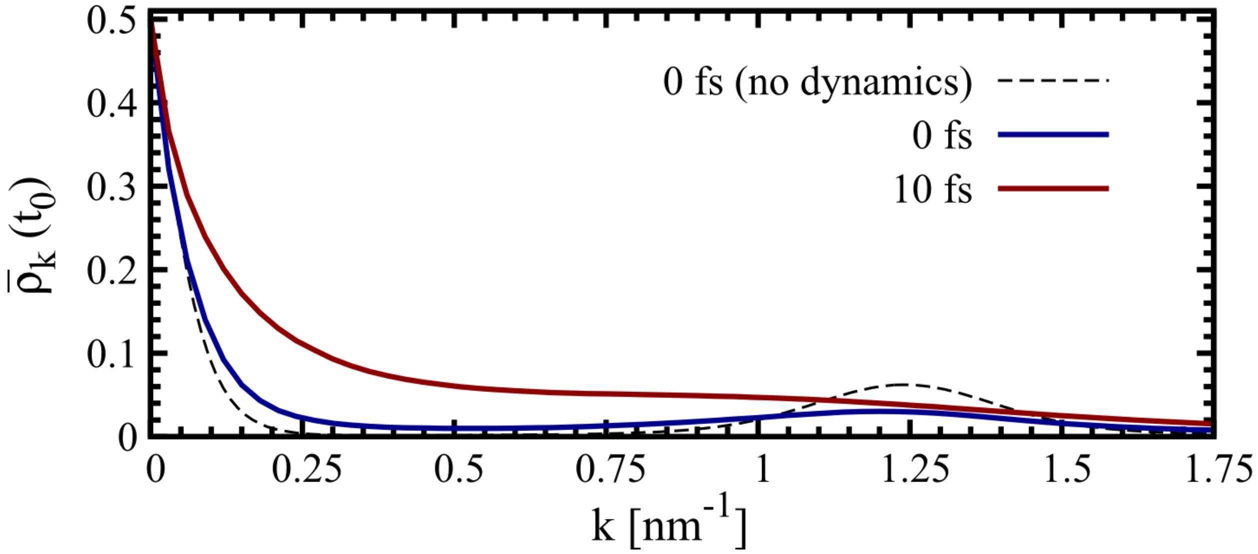

- Significant **relaxation** takes place already **during** the excitation **pulse**
- Carrier-carrier and carrier-phonon scattering are in direct **competition**

Thermalization

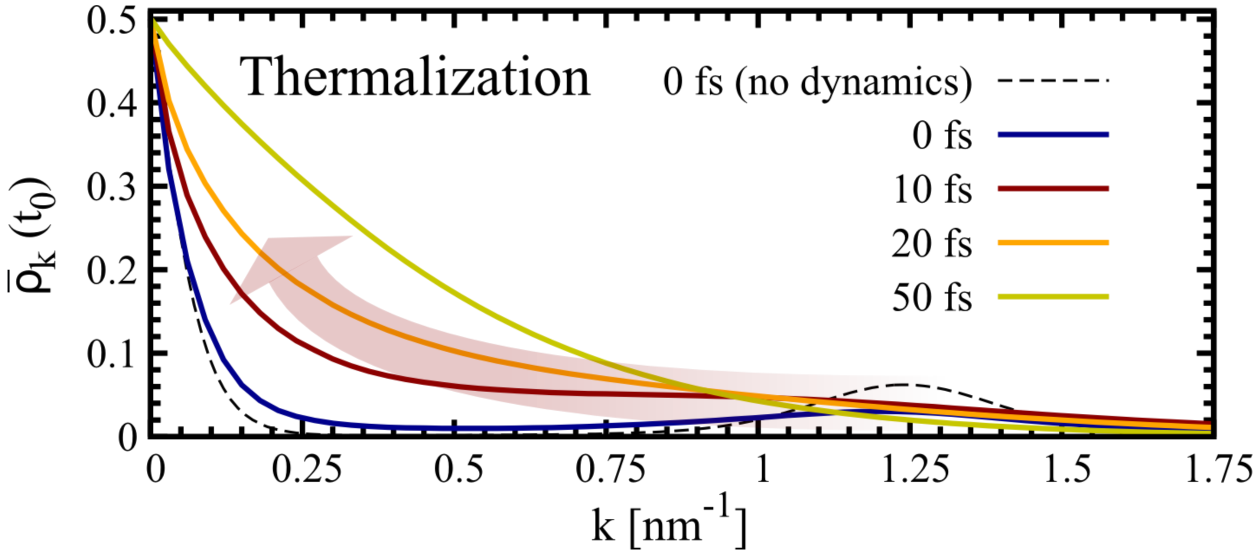

- Significant **relaxation** takes place already **during** the excitation **pulse**
- Carrier-carrier and carrier-phonon scattering are in direct **competition**
- **Thermalized distribution** reached within the first **50-100 fs**

PRB 84, 205406 (2011)

Carrier cooling

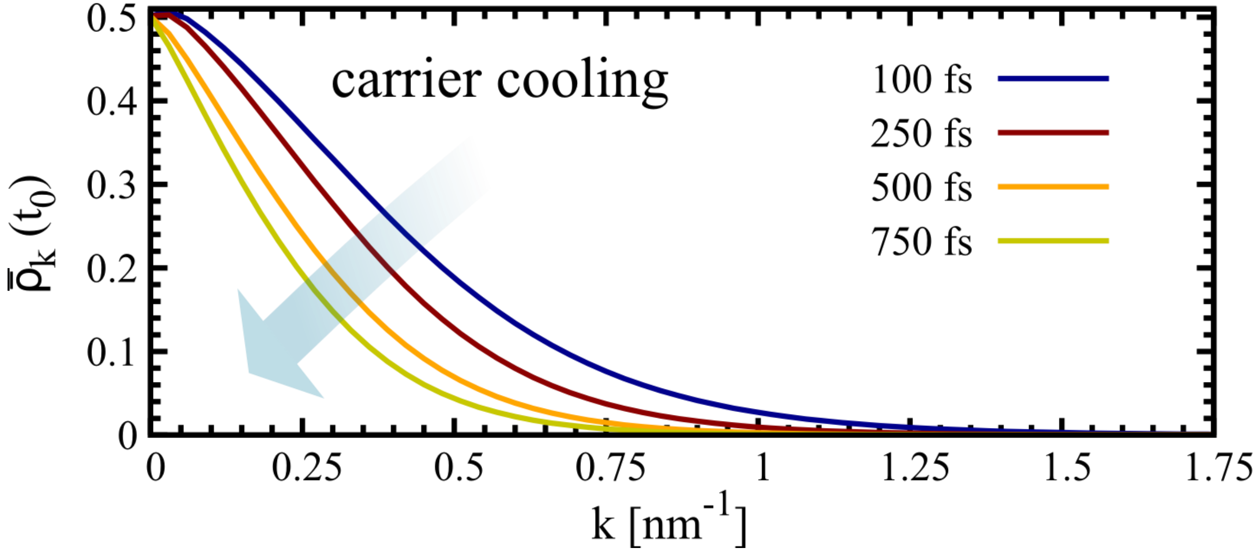

- **Carrier cooling** takes place on a **picosecond time scale**
- **Optical phonons** (in particular ΓLO, ΓTO and K phonons) are more **efficient** than acoustic phonons

PRB 84, 205406 (2011)

Carrier dynamics

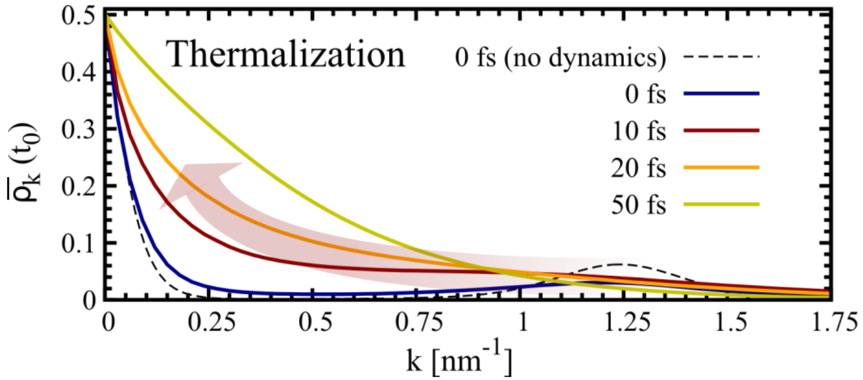

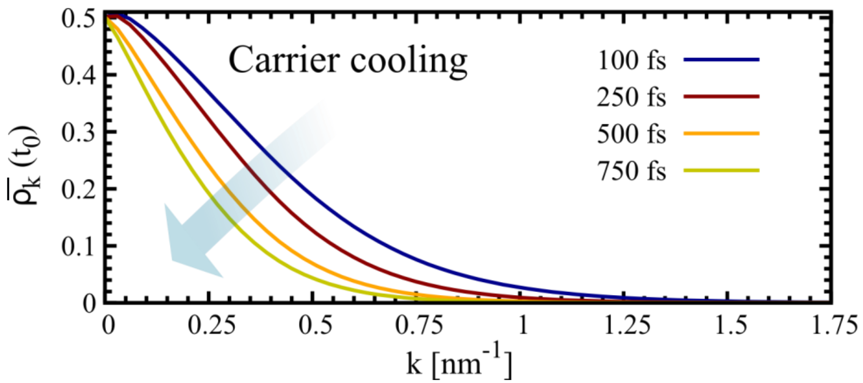

Carrier dynamics is characterized by **two processes**:

→ Carrier-carrier and carrier-phonon scattering leads to **thermalization** on **fs time scale**

→ Phonon-induced **carrier cooling** occurs on **ps time scale**

PRB 84, 205406 (2011)

Nano Lett. 10, 4839 (2010)

Experiment in the infrared regime

- **High-resolution pump-probe-** experiment to measure differential transmission in graphene
- **Excitation energy** in the infrared region at **1.5 eV**
- Temporal **resolution** is **10 fs**
- Initial increase of transmission is due to the **absorption bleaching**
- Flowing **decay** is characterized by **two time constants**:

$\tau_1 = 140$ fs; $\tau_2 = 0.8$ ps

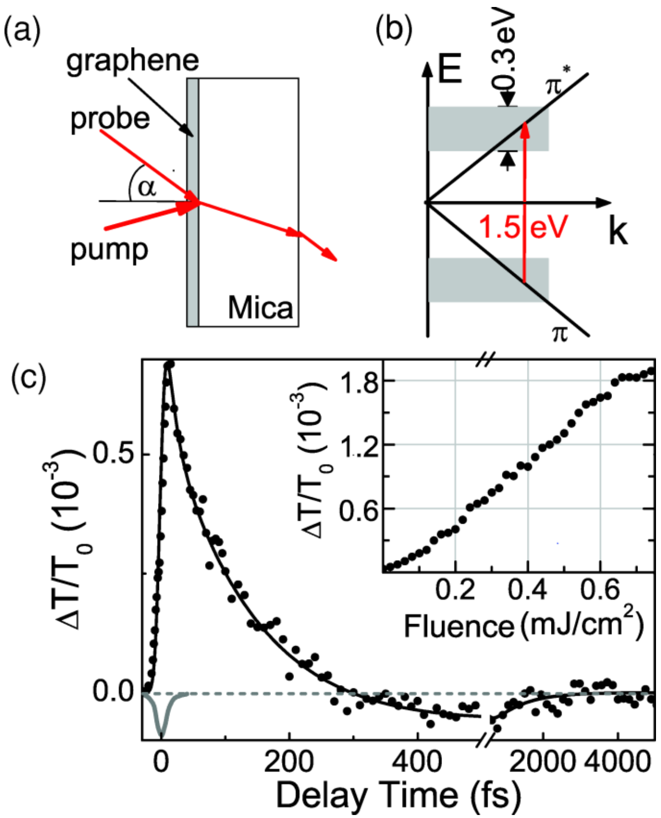

T. Elsaesser (Max-Born Institut, Berlin)

PRB 83, 153410 (2011)

Theory-experiment comparison

Experiment

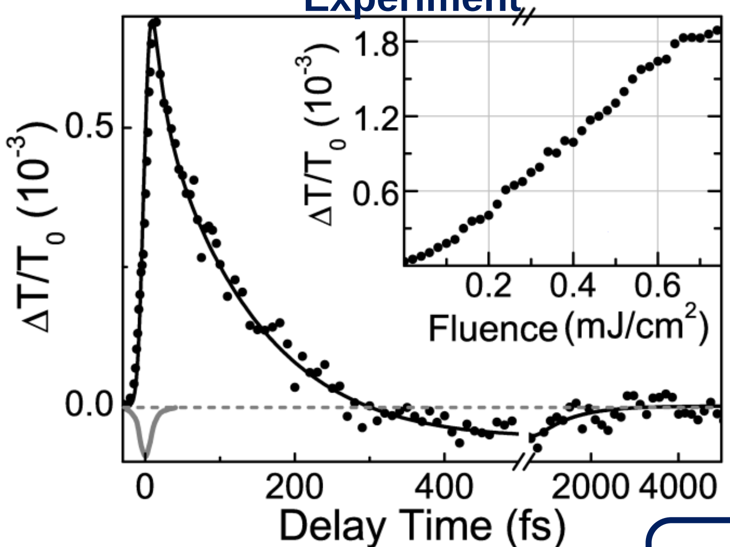

τ_1 = 140 fs; τ_2 = 800 fs

Two time constants

Theory

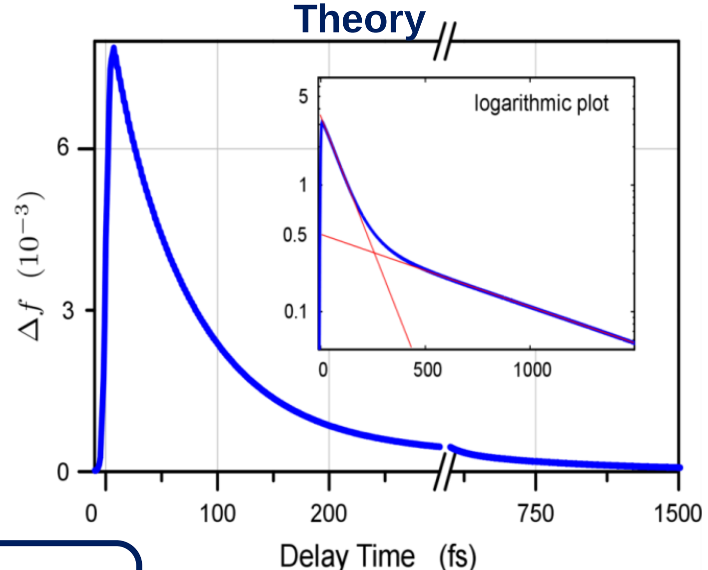

τ_1 = 104 fs; τ_2 = 709 fs

- Theory is in **good agreement** with experiment:
  τ_1 corresponds to **thermalization**, τ_2 described **carrier cooling**
- Observed **negative DTS** still under debate in literature

→ **Challenge: Impact of the substrate**

PRB 83, 153410 (2011)

Outline

- Anisotropy, thermalization, and cooling
- Auger-induced carrier multiplication
- Transient optical gain

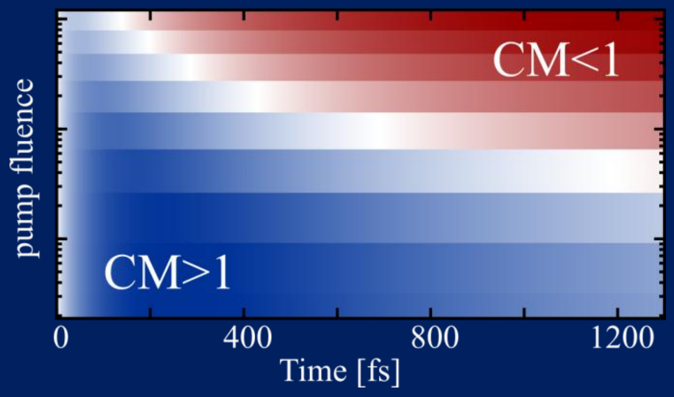

Auger scattering

- Auger scattering **changes** the number of charge **carriers in the system**

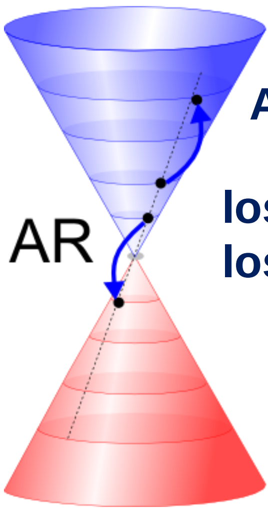

Auger recombination (AR)

lost electron in cond.band
lost hole in valence band

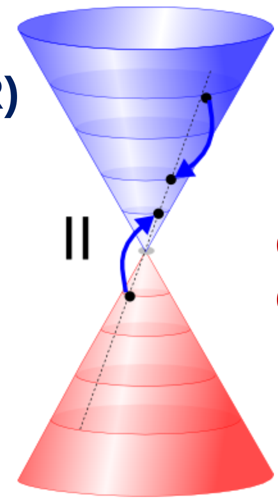

Inverse Auger recombination or **impact ionization (II)**

gained electron in cond. band
gained hole in valence band

Impact ionization

- Auger scattering **changes** the number of charge **carriers in the system**

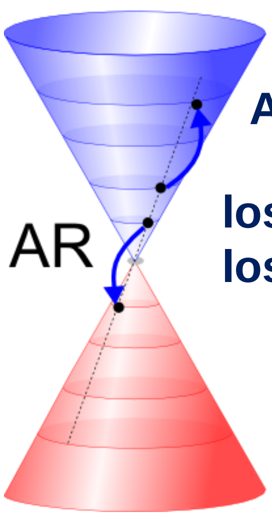

Auger recombination (AR)

lost electron in cond.band
lost hole in valence band

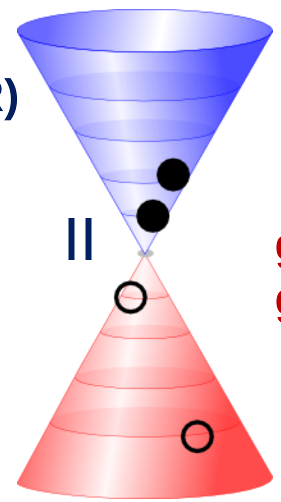

Inverse Auger recombination or **impact ionization (II)**

gained electron in cond. band
gained hole in valence band

→ **carrier multiplication**

- In **conventional semiconductors** (band gap, parabolic band structure) Auger scattering is **inefficient** due to energy and momentum conservation

And in graphene?

Carrier density

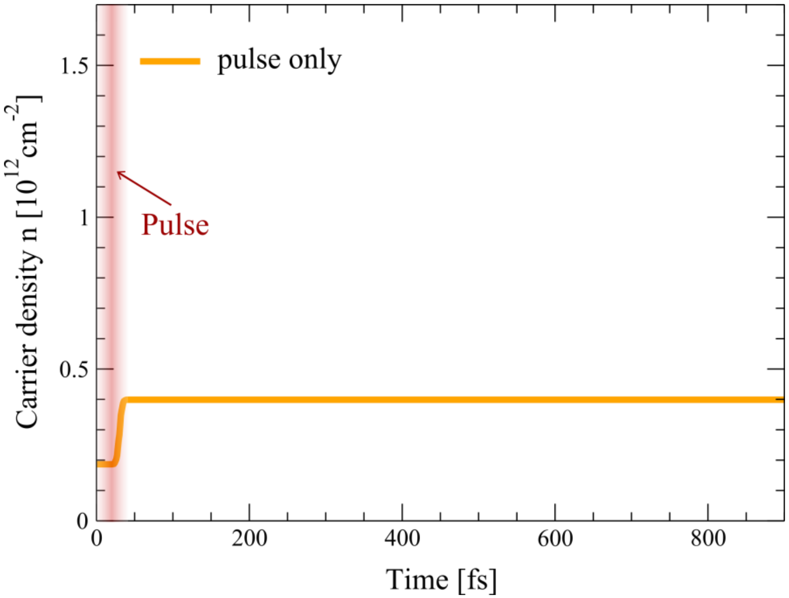

- **Carrier density increases** during the excitation pulse

Carrier multiplication

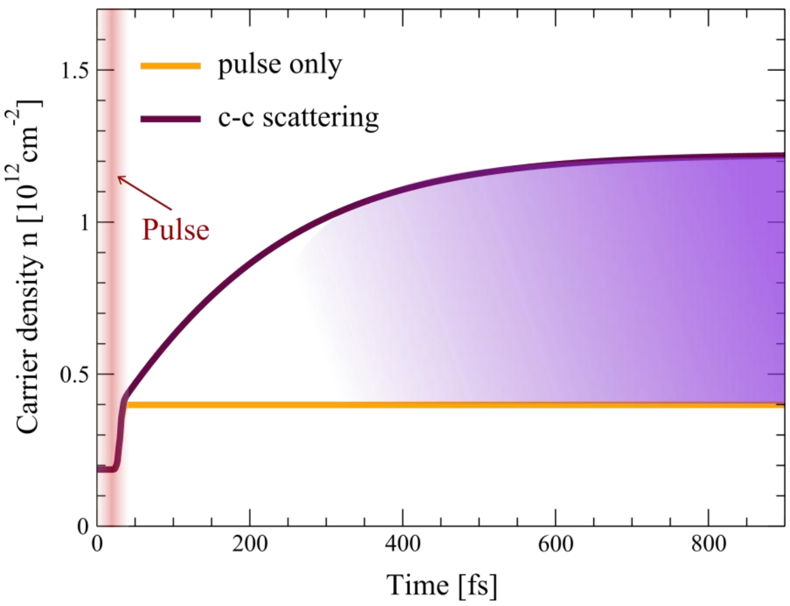

- Auger scattering leads to **carrier multiplication (CM)**

Nano Lett. 10, 4839 (2010)

Carrier multiplication

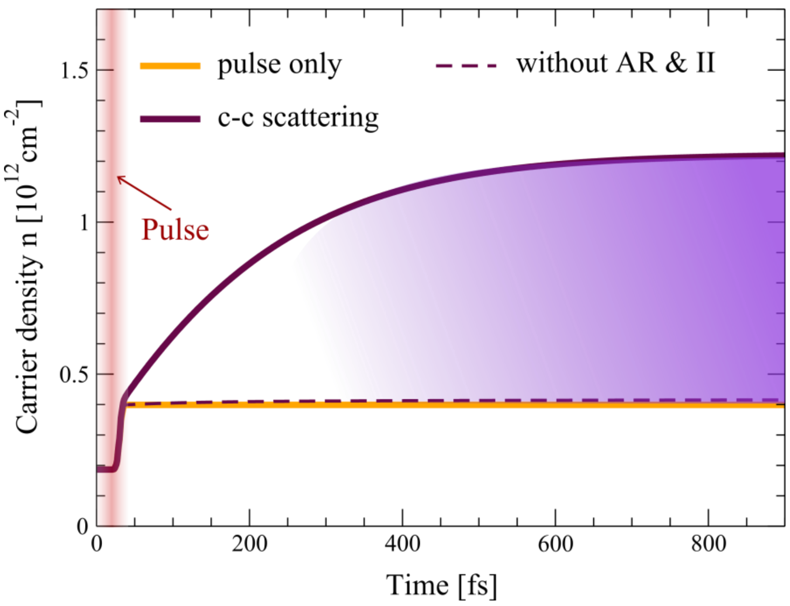

- Auger scattering leads to **carrier multiplication (CM)**

Nano Lett. 10, 4839 (2010)

Carrier multiplication

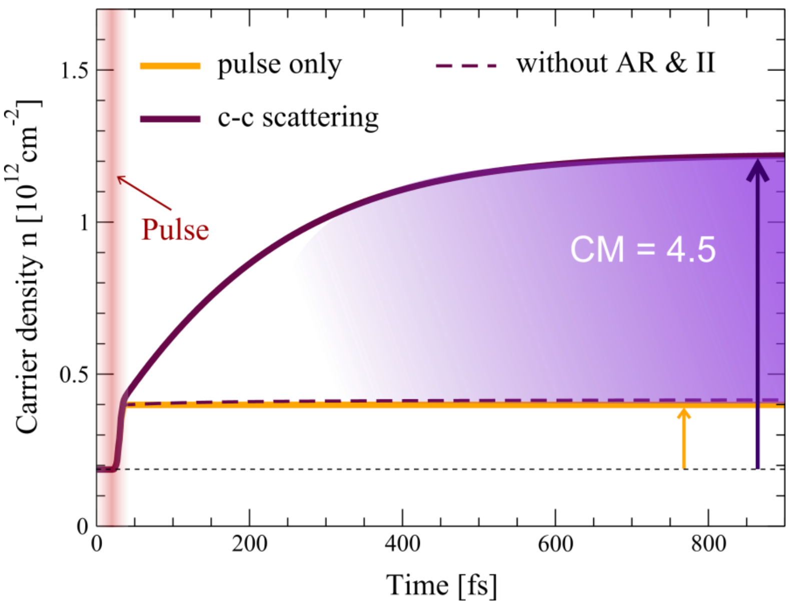

- Auger scattering leads to **carrier multiplication (CM)**
- **Asymmetry** between II and AR **in favor** of **impact ionization (II)**

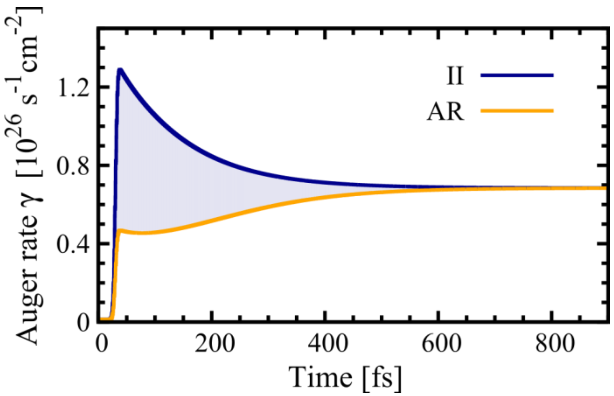

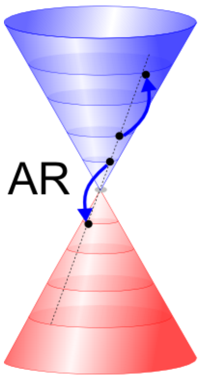

Nano Lett. 10, 4839 (2010)

Impact of phonons

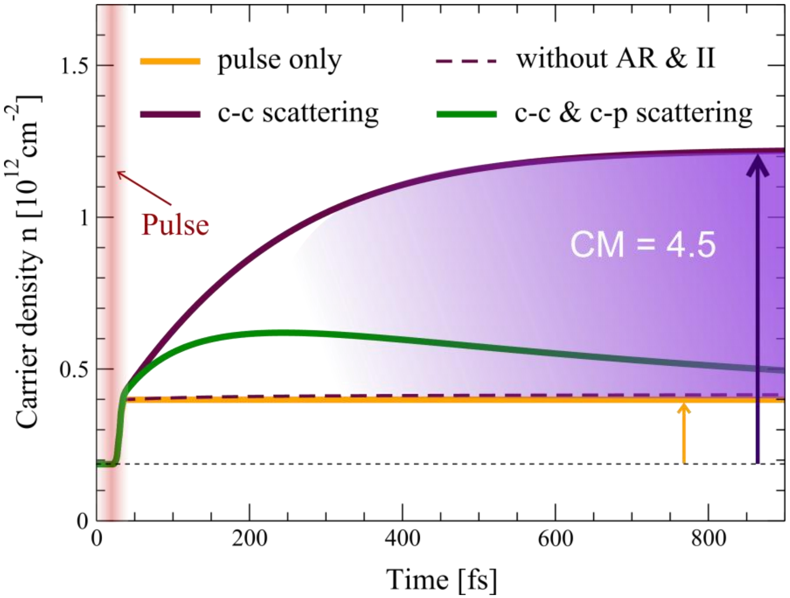

- Auger scattering leads to **carrier multiplication (CM)**
- **Asymmetry** between II and AR **in favor** of **impact ionization (II)**

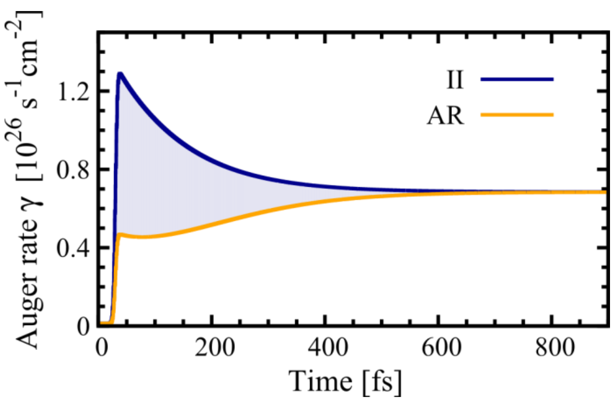

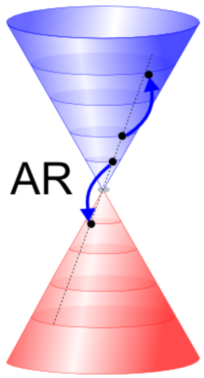

- Carrier-**phonon** scattering **reduces** CM on a **ps time scale**

Nano Lett. 10, 4839 (2010)

Carrier multiplication

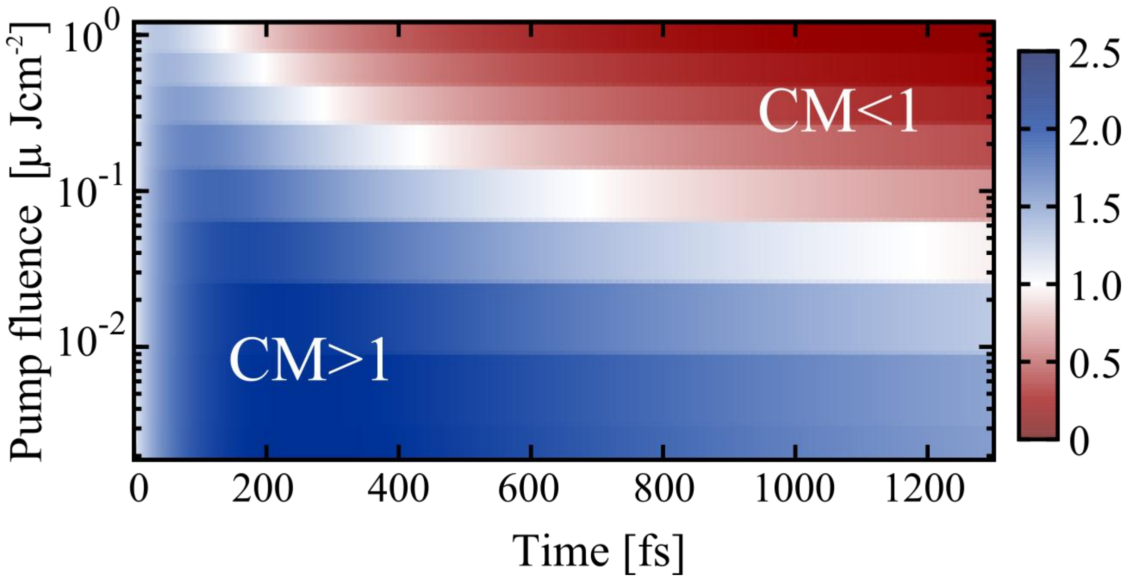

- Carrier multiplication shows a clear **dependence** on the **pump fluence**
- Two regions with CM > 1 and CM < 1 with **phonon-induced cross-over**
- CM remains **stable** on a **ps time scale** ⟶ **application** potential

⟶ **Experimental confirmation** of CM by Kurz (RWTH Aachen)

PRB Rapid 85, 241404(R) (2012)

Outline

- Anisotropy, thermalization, and cooling
- Auger-induced carrier multiplication
- Transient optical gain

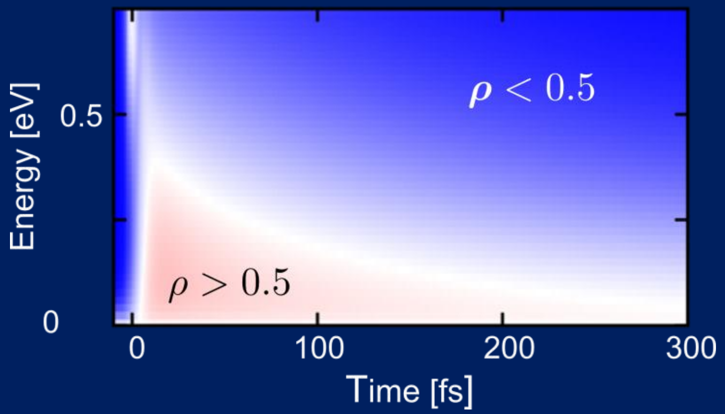

Transient population inversion

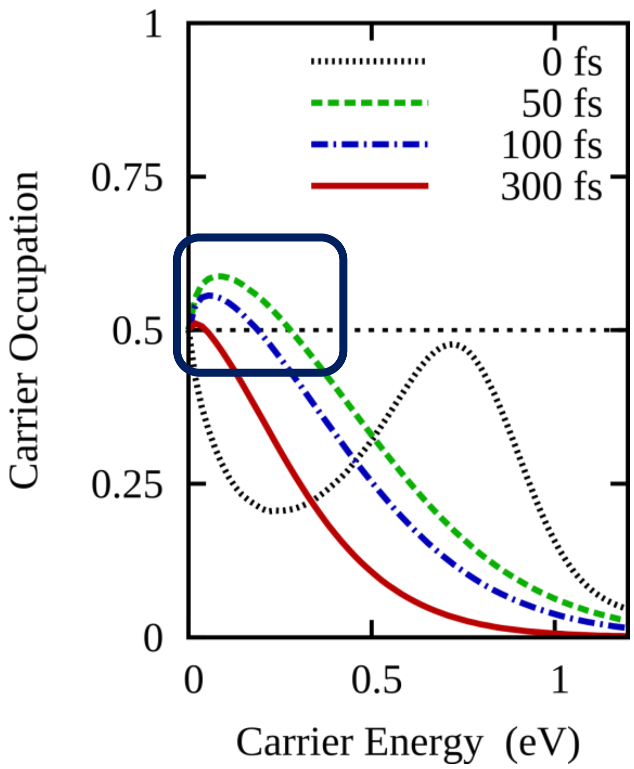

- **Population inversion** occurs in the **high-excitation** regime (>0.2 $mJcm^{-2}$)
- **Spectrally** and **temporally limited** depending on pump fluence

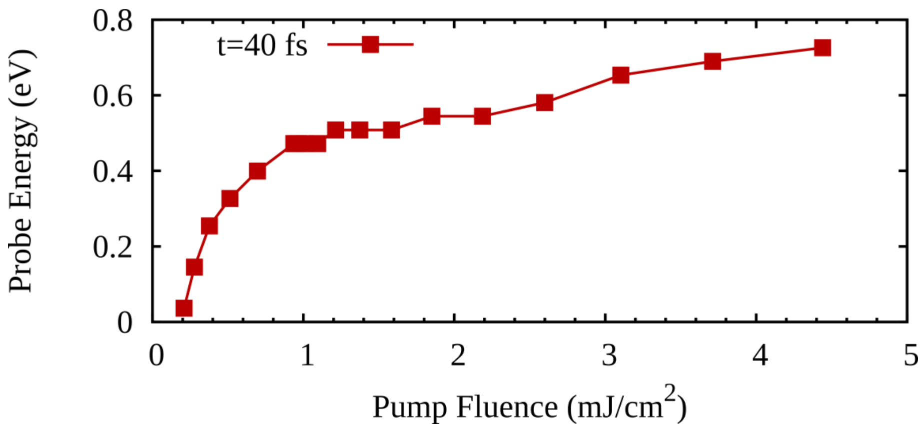

Transient population inversion

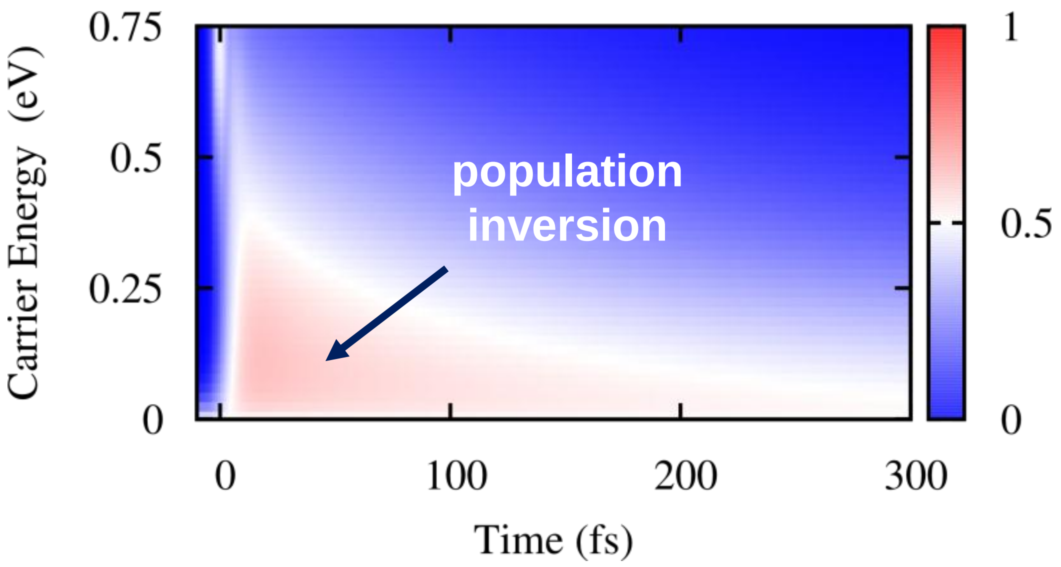

- For a pump fluence of **2.5 mJcm^{-2},** population **inversion** found in the first **300 fs** up to a carrier energy of **400 meV**

→ **Good agreement** with a recent **experiment:** *PRL 108, 167401 (2012)*

Optical gain manifested in **negative conductivity** (fluences > 2 mJcm^{-2}, first 200 fs, energy up to 550 meV)

arXiv: 1209.4833 (2012)

Impact of phonons

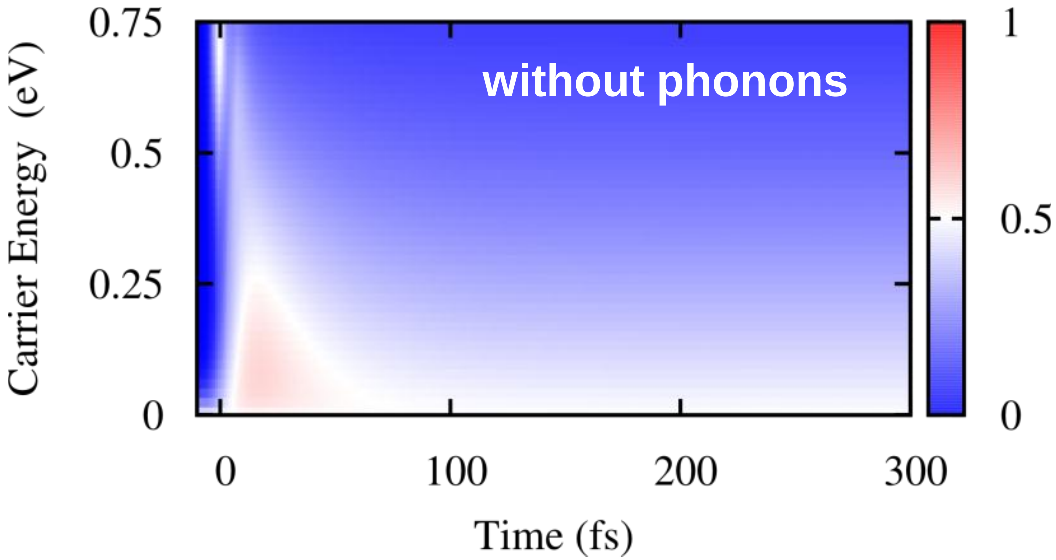

- For a pump fluence of **2.5 mJcm^{-2},** population **inversion** found in the first **300 fs** up to a carrier energy of **400 meV**

- **Intraband** scattering with **phonons** plays a crucial role: the gain region is strongly reduced without phonons

arXiv: 1209.4833 (2012)

Microscopic mechanism

- Excited carriers scatter down via **phonon-induced intraband** processes

- **Vanishing density of states** at the Dirac point → **population inversion**

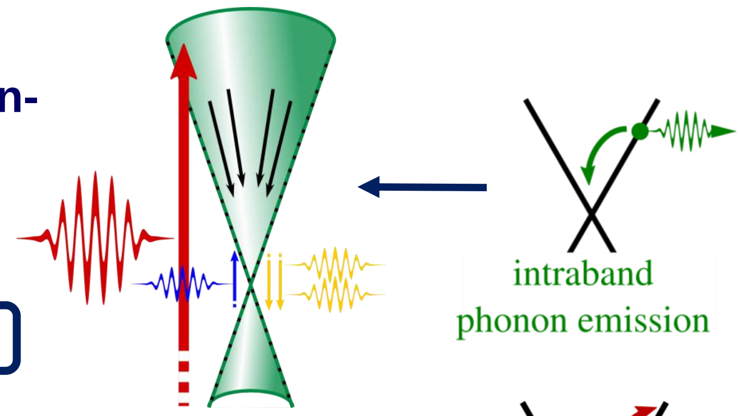

- Efficient **Auger recombination** and **phonon-induced interband** scattering give rise to a **fs-decay** of the population inversion

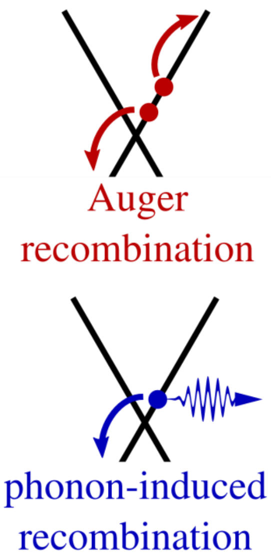

arXiv: 1209.4833 (2012)

Relaxation dynamics in graphene

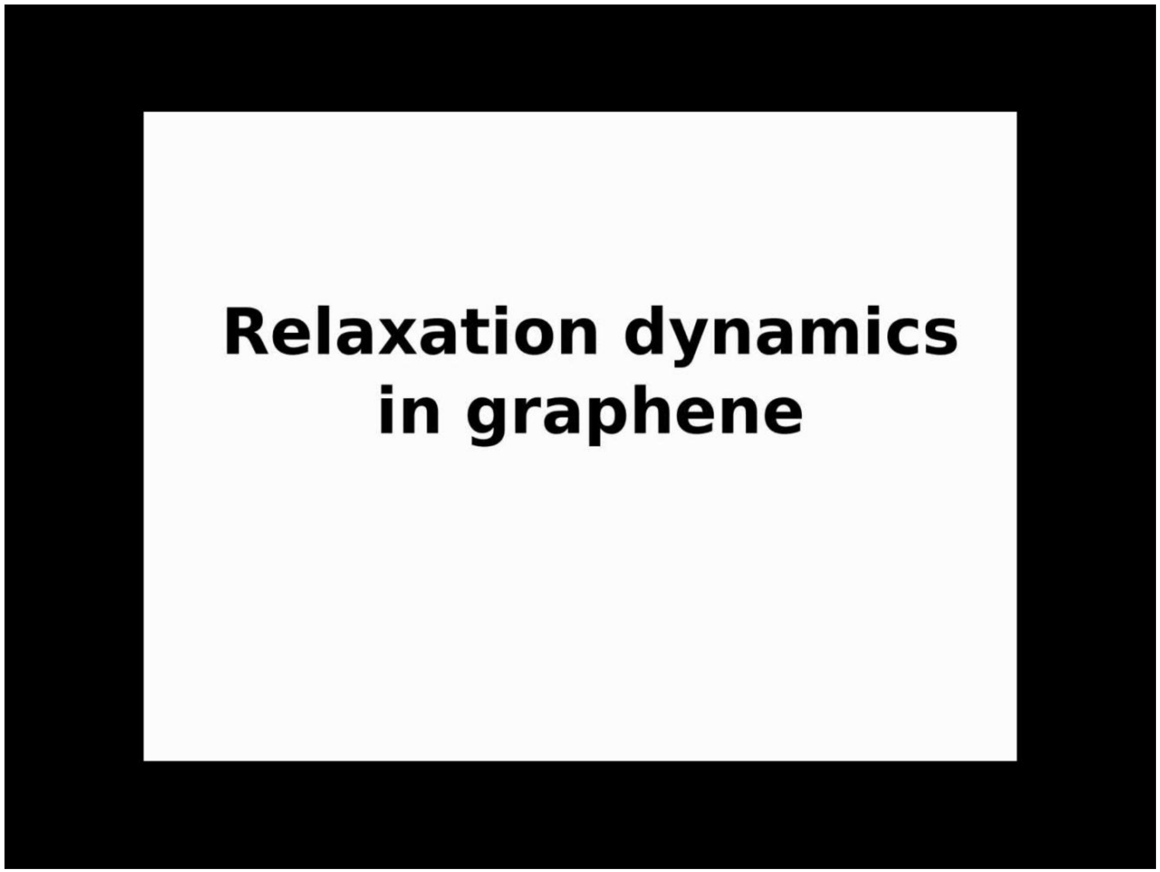

Future challenges

- **Non-Markov** relaxation dynamics including **quantum-kinetic memory effects**

  Calculations for CNTs reveal **oscillations** in occupation

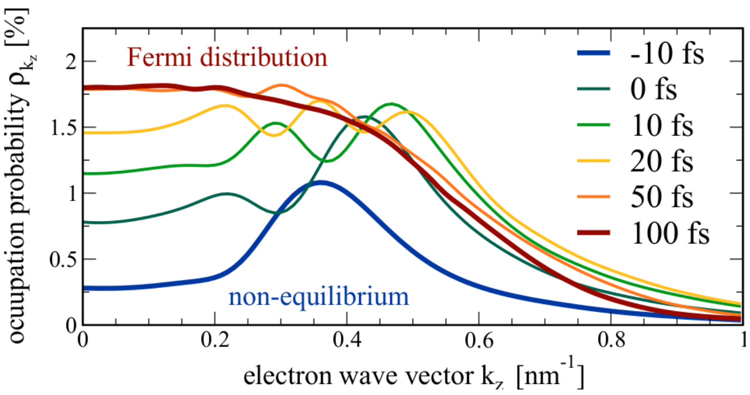

- **Impact of the substrate** is unknown and so far widely neglected in literature

- Number of relaxation channels strongly reduced close to Dirac point

  Prediction of “supercollisions“: **disorder-assisted carrier-phonon** scattering